

Calculations of PKA spectra and kerma factors using PHITS code
and measurement of displacement cross section of Cu irradiated
with 125 MeV protons at cryogenic temperature

Yosuke Iwamoto

Nuclear Science and Engineering Center
Japan Atomic Energy Agency



(1) Calculations of PKA spectra using PHITS-EG for 5 and 14.5 MeV neutrons

(2) Calculations of neutron kerma factors using PHITS-EG with $1e-10 < E_n < 20$ MeV

(3) Calculation of gas production cross sections for p+Fe using PHITS

(4) Measurement of displacement cross section of copper irradiated with 125 MeV protons

(1) Calculation of PKA spectra using PHITS-EG and NJOY-SPKA

Neutron energy (MeV)	Target	Processing step	ACE Library
5, 14.5	^{28}Si , ^{56}Fe , ^{90}Zr , ^{184}W	PHITS-EG	JENDL-4
		PHITS-EG	ENDF/B-VII.1
		NJOY-SPKA	JENDL-4
		NJOY-SPKA	ENDF/B-VII.1

Energy group structure of neutron and PKA is [vitamin-j 175-group](#).

NJOY-SPKA: PKA matrixes are produced by NJOY and then fold with neutron spectrum using SPKA code.

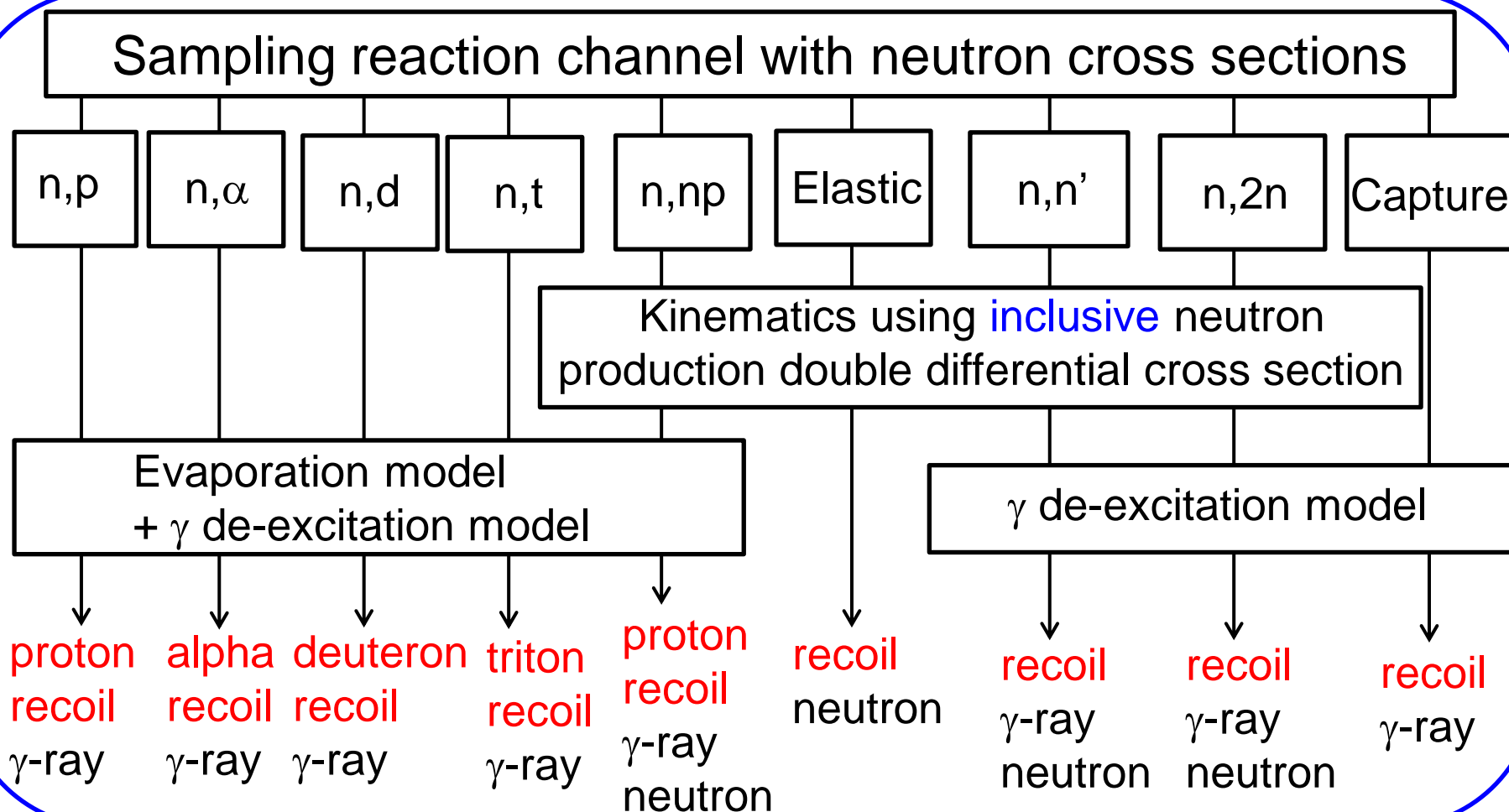
Obtained from <https://www-nds.iaea.org/CRPdpa/>

Next slide: PHITS-EG (Event Generator mode)

Event generator mode by neutrons with $E_n < 20$ MeV

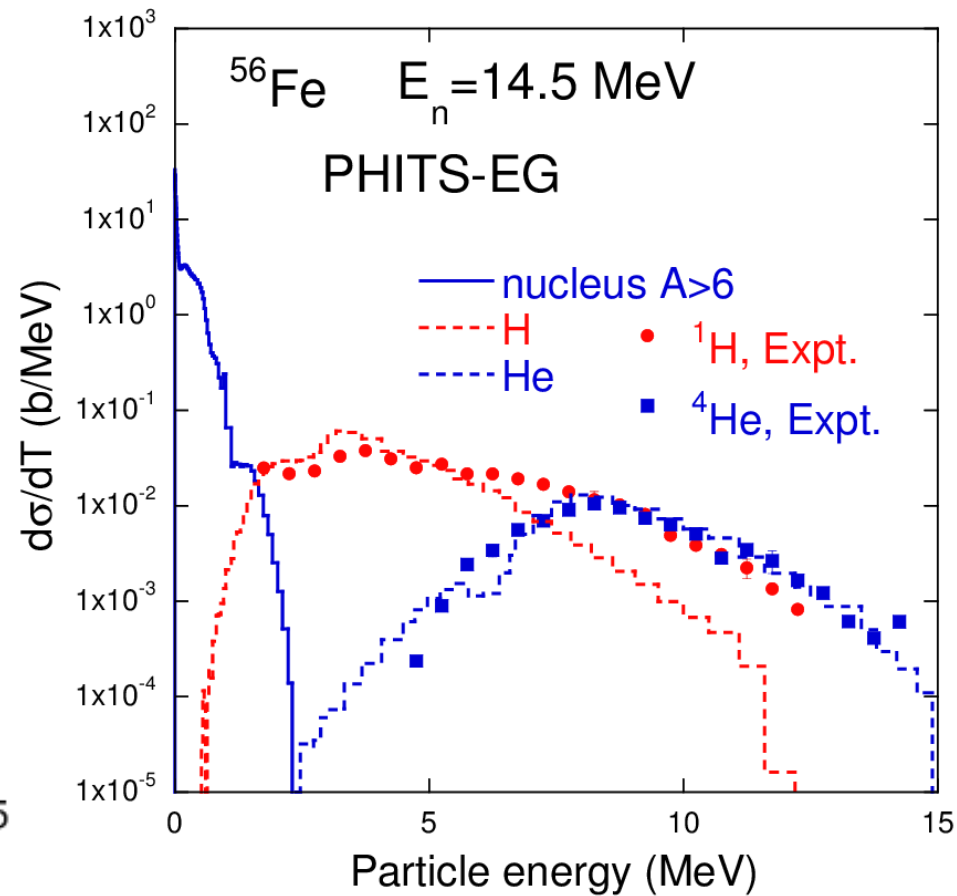
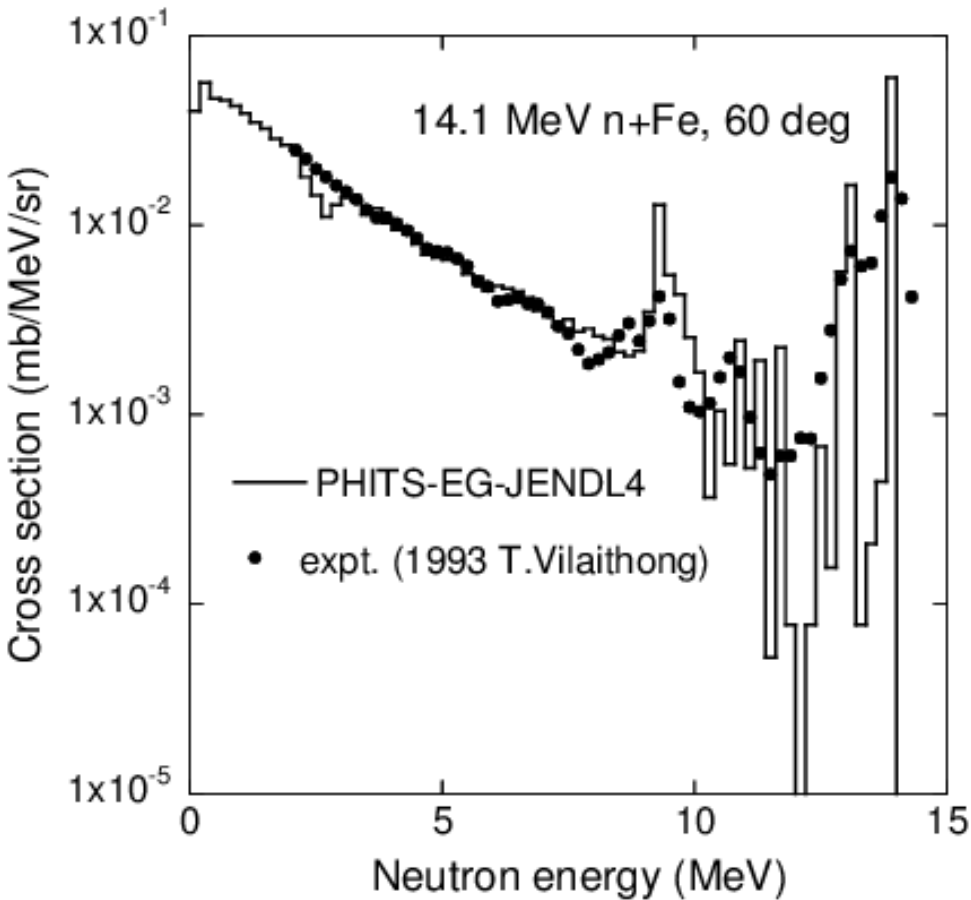
The model can determine all ejectiles with keeping energy and momentum conservation.

T. Ogawa et al., NIM A 763 (2014) 575-590.



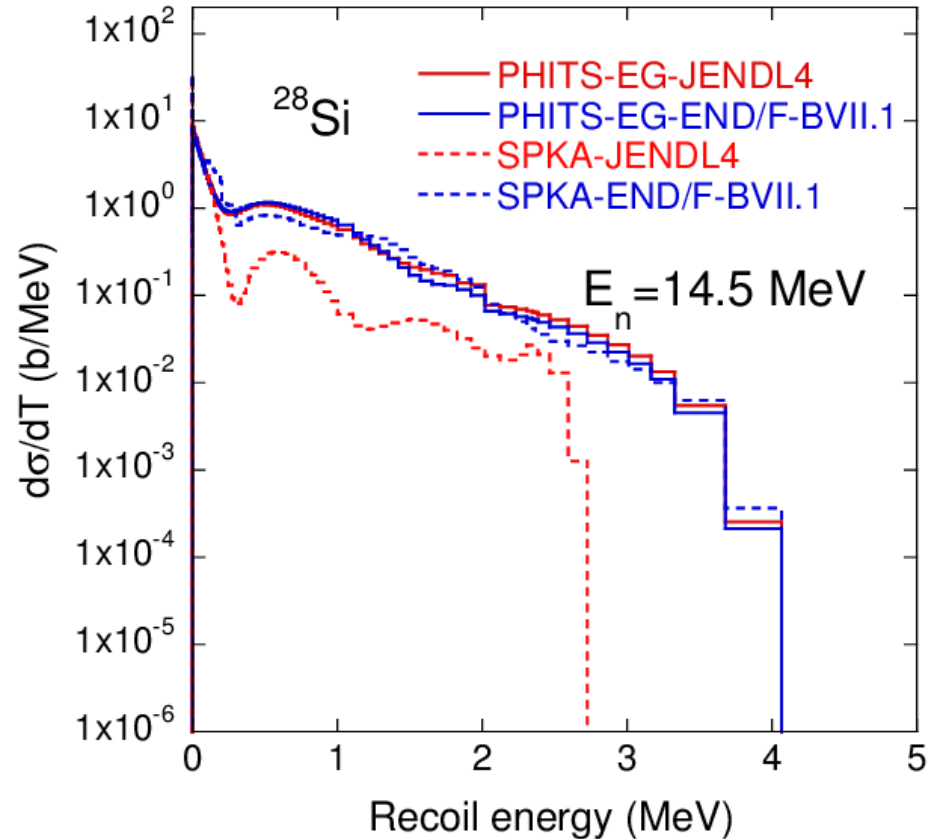
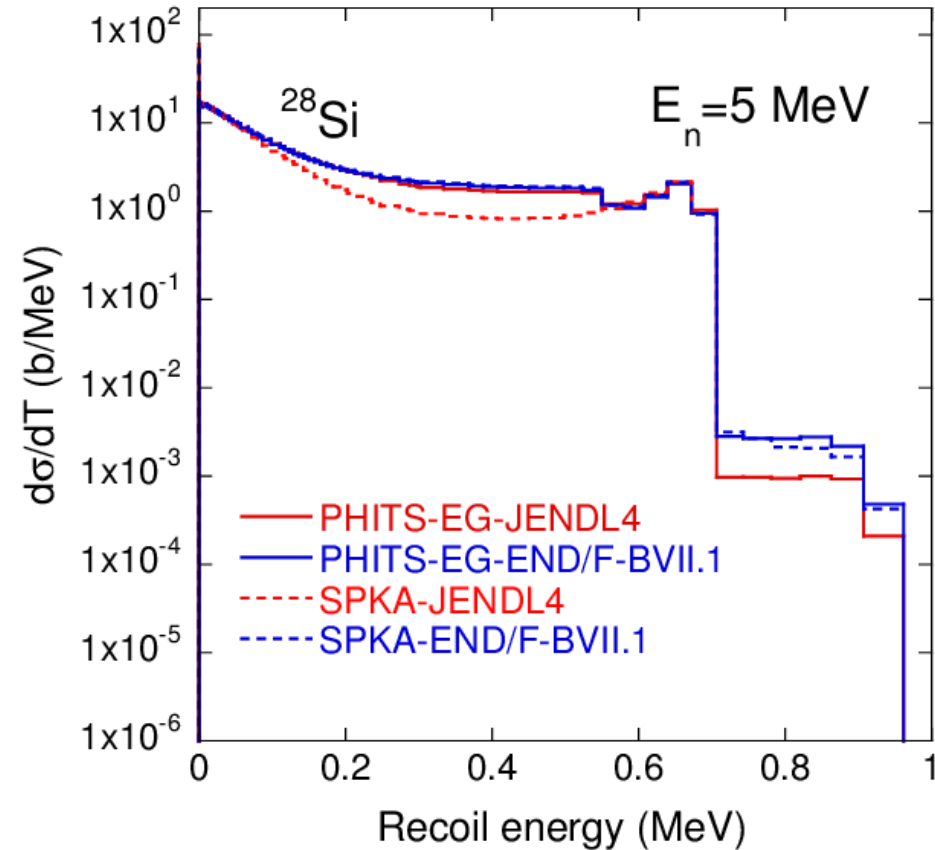
PHITS-EG uses **inclusive** (n,n') cross sections with residuals in all excited states and in continuum.

Benchmark calculation for PHITS-EG



PHITS-EG can reproduce neutron and α energy spectra, but it overestimates the experimental data for proton over 5 MeV.

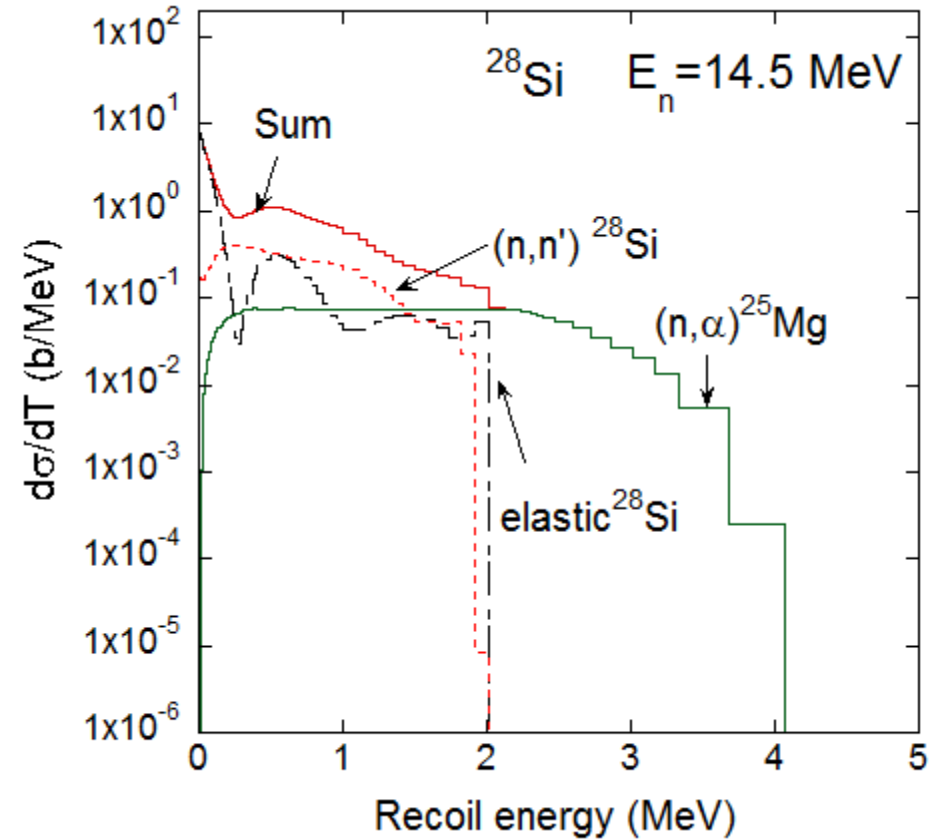
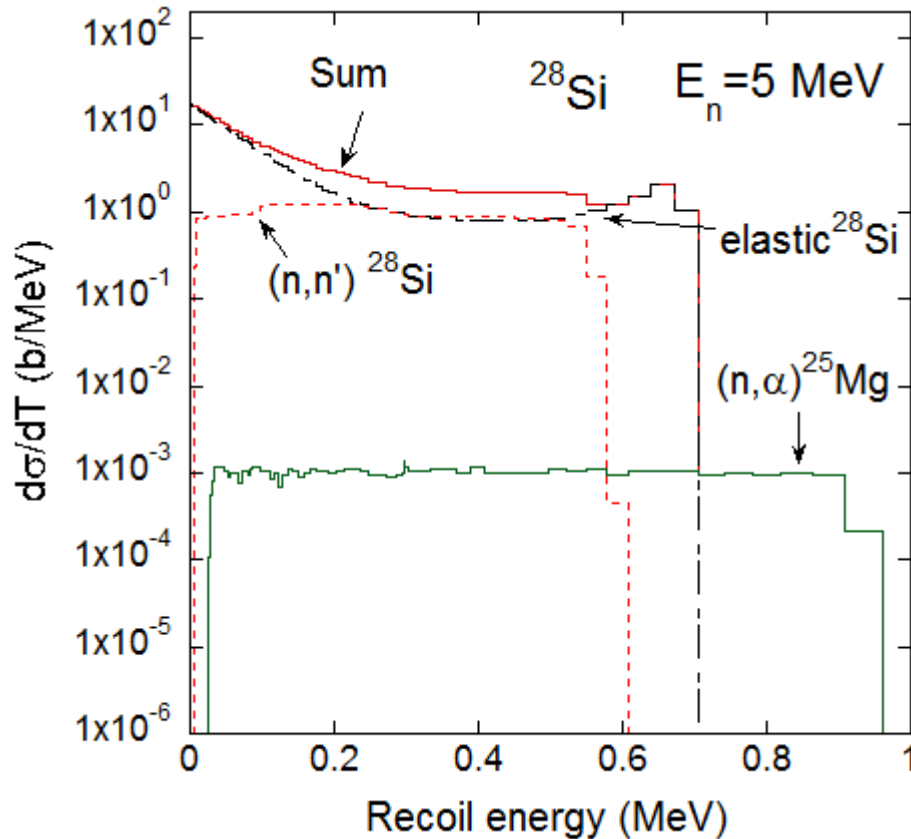
PKA spectra for n+Si



- ✓ PKA spectra processed by SPKA-JENDL4 are not correct due to lack of recoil data in JENDL4.
- ✓ Good agreements between PHITS-EG and SPKA-END/F-BVII.1

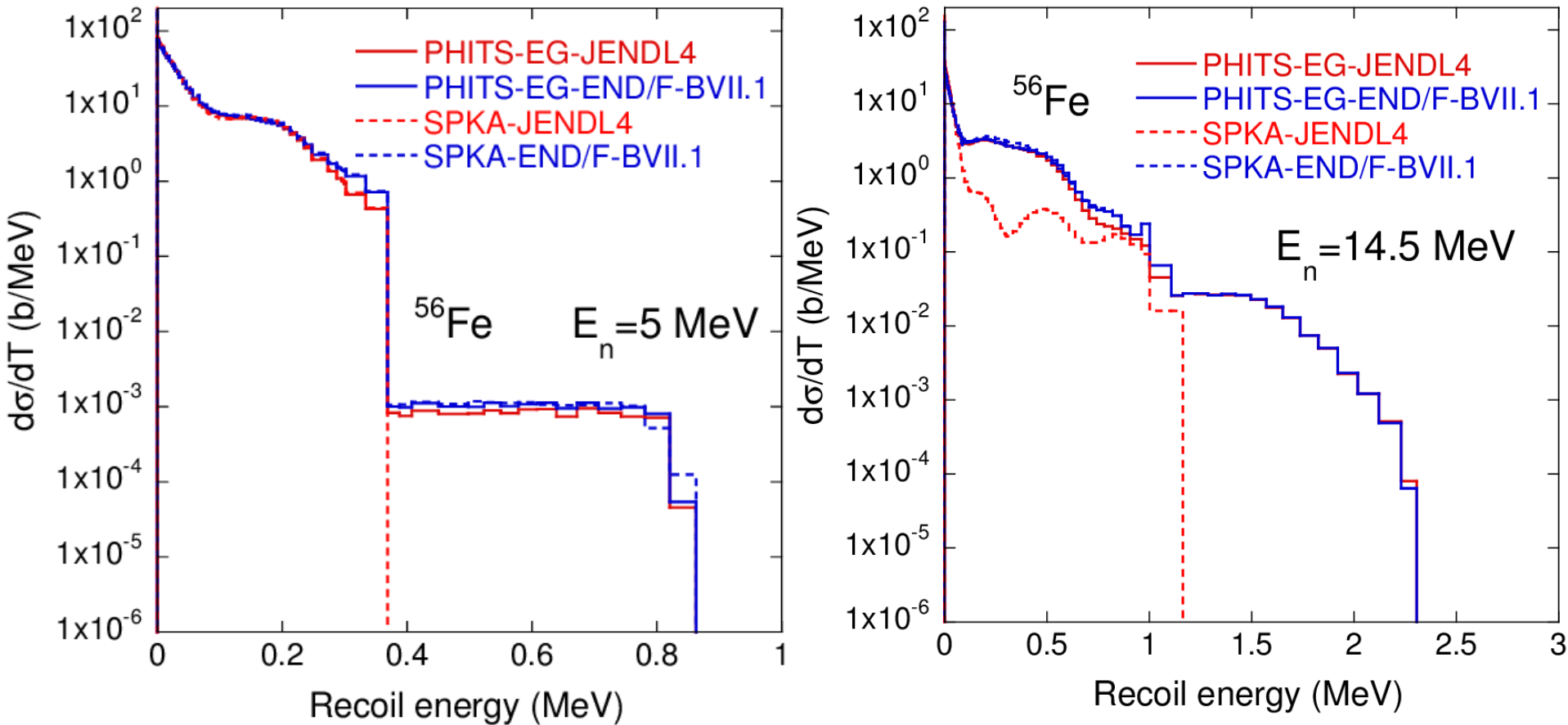
PKA spectra for n+Si

Contribution of reaction channel to total using PHITS-EG-JENDL4.



5 MeV: Contribution of elastic and (n, n') on PKA spectra are large.
14.5 MeV: (n, α) is dominant for higher energy region.

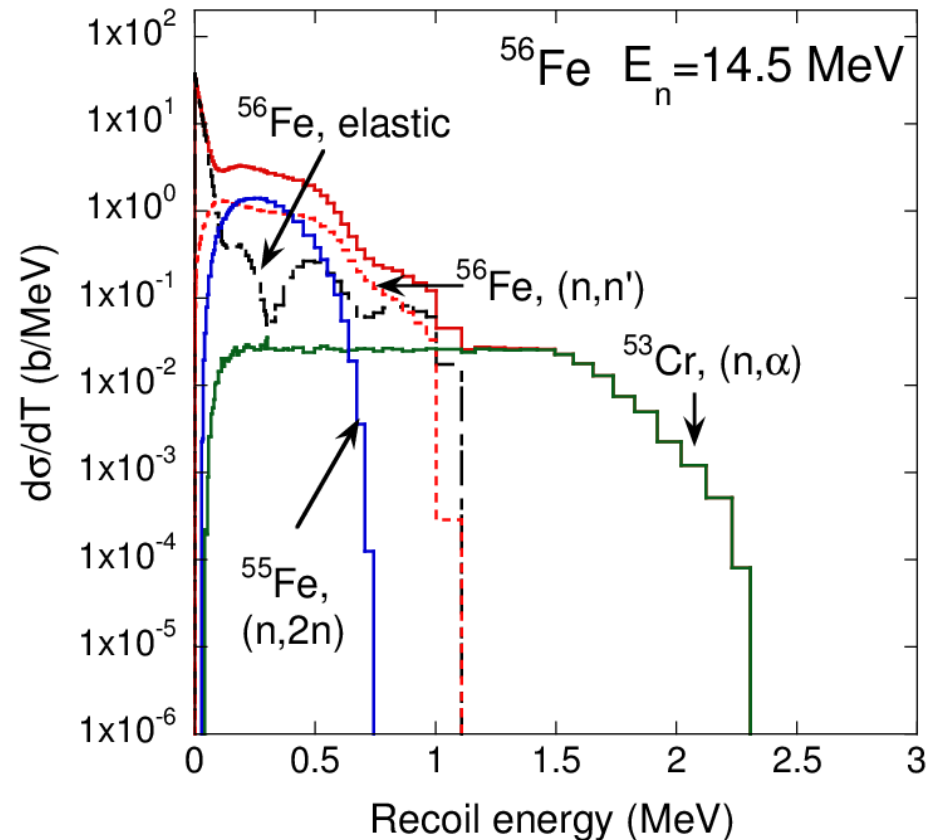
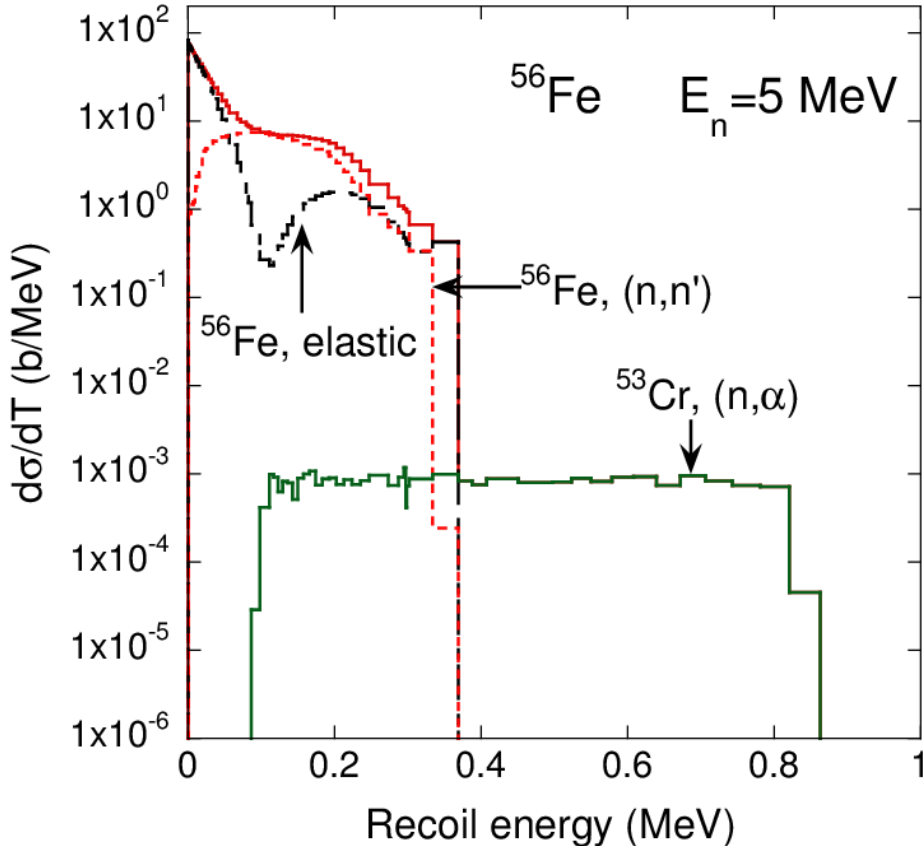
PKA spectra for n+Fe



PKA spectra processed by SPKA-JENDL4 are not correct due to lack of recoil data in JENDL4.

PKA spectra for n+Fe

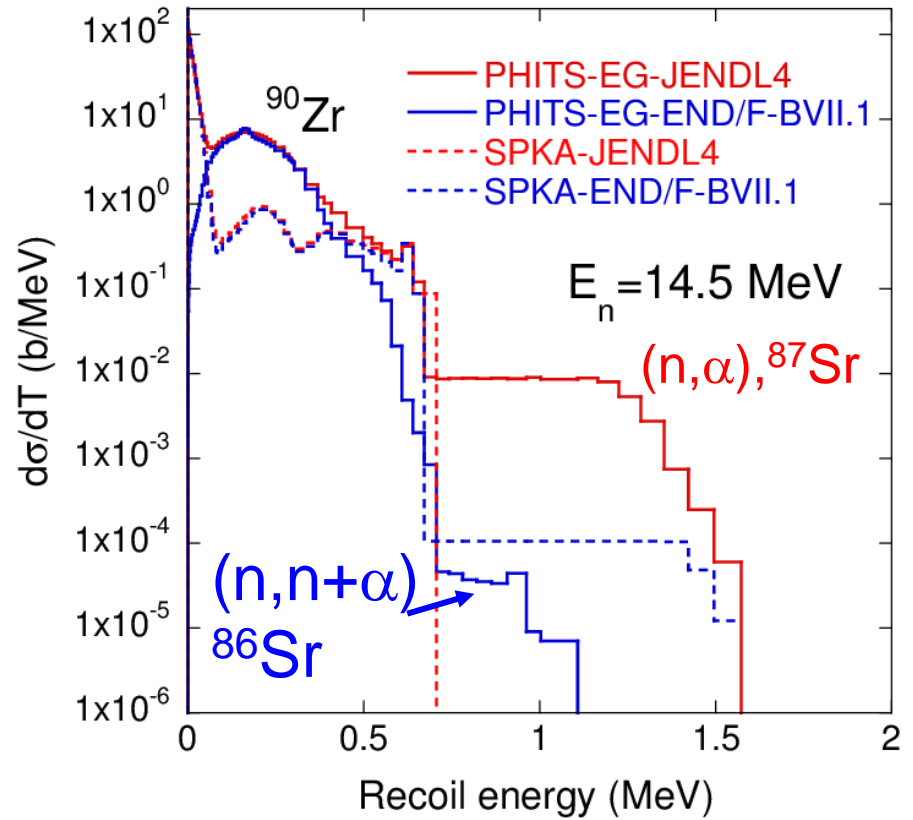
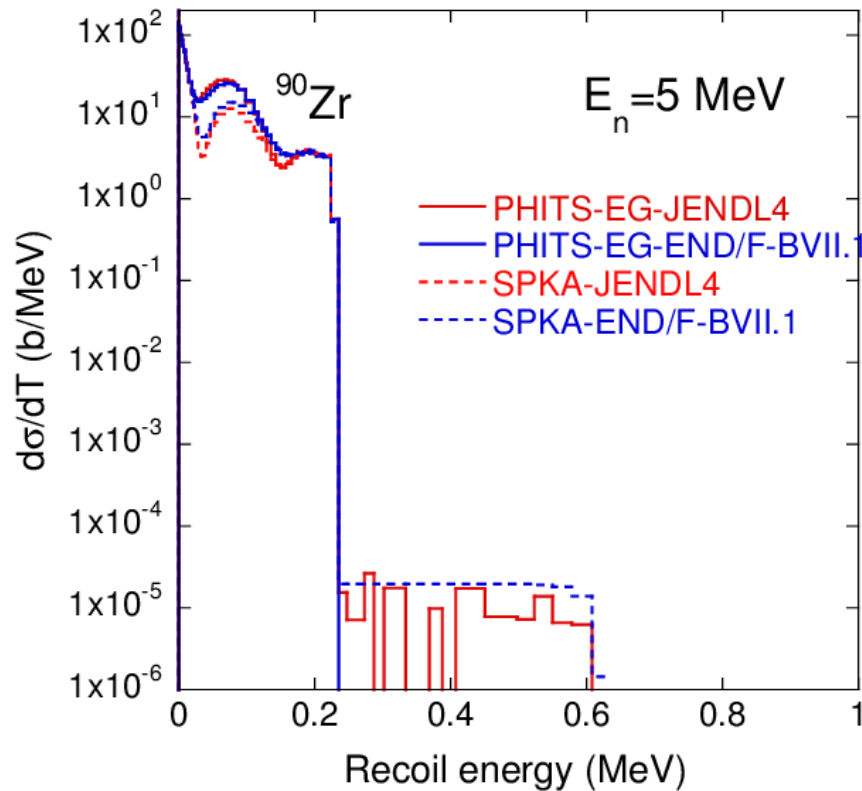
Contribution of reaction channel to total using PHITS-EG-JENDL4.



5MeV: Contribution of elastic and (n,n') on PKA spectra are large.

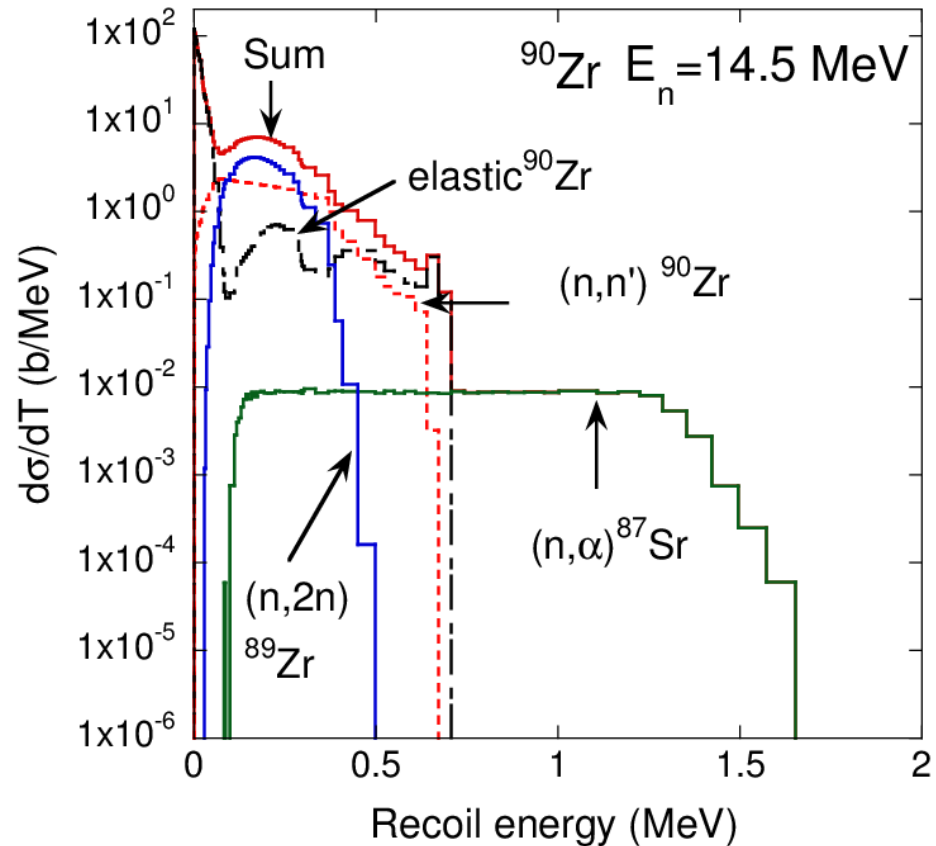
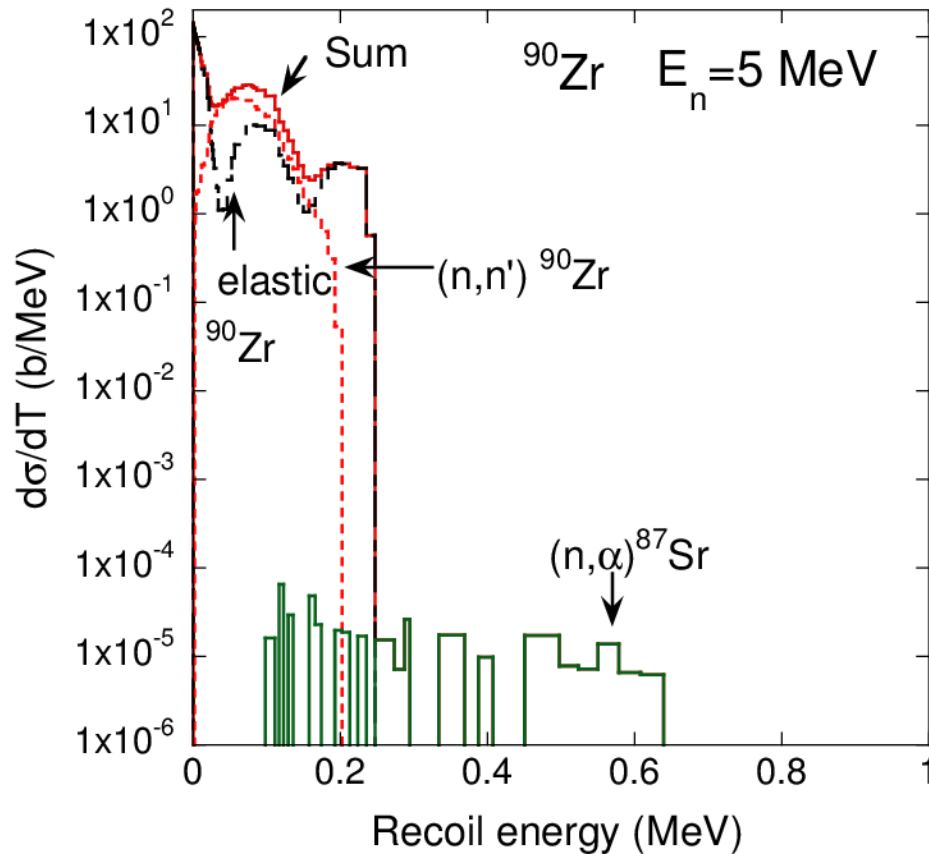
14.5MeV: Contribution of (n,2n) is also large. (n, α) is dominant for higher energy.

PKA spectra for n+Zr



PKA spectra for n+Zr

Contribution of reaction channel to total using PHITS-EG-JENDL4.

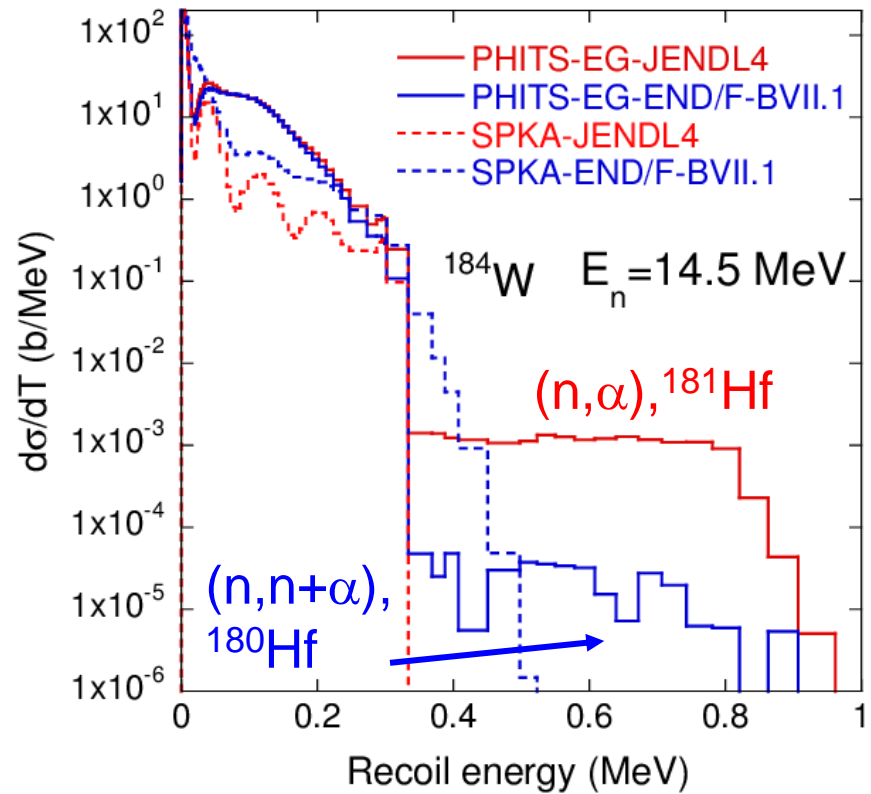
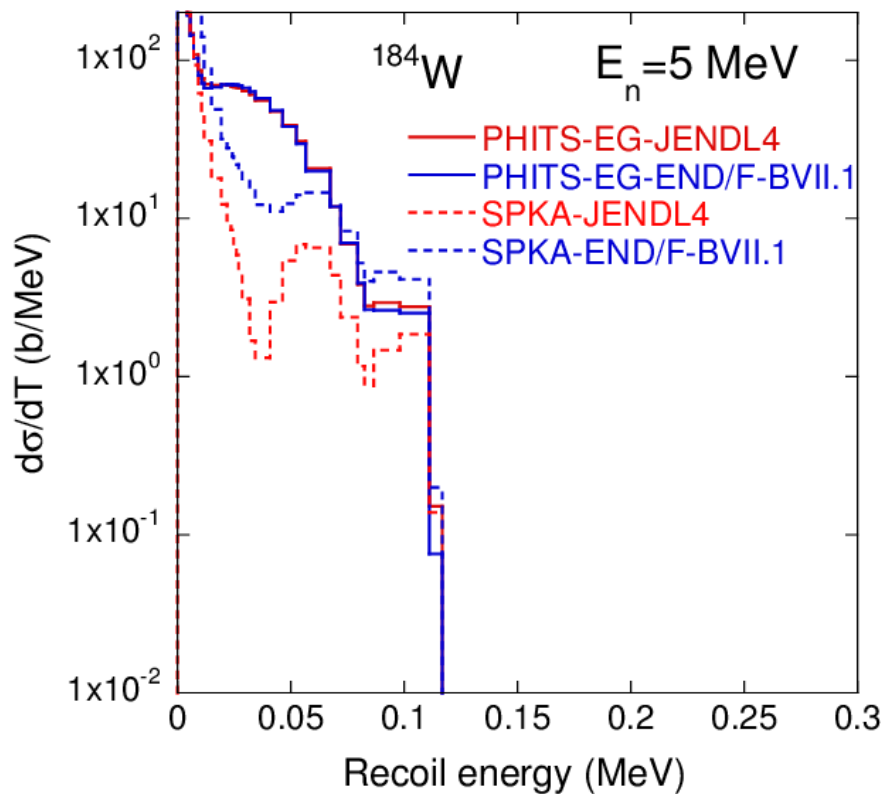


5MeV: Contribution of elastic and (n,n') on PKA spectra are large.

14.5MeV: Contribution of $(n,2n)$ is also large. (n,α) is dominant for higher energy.

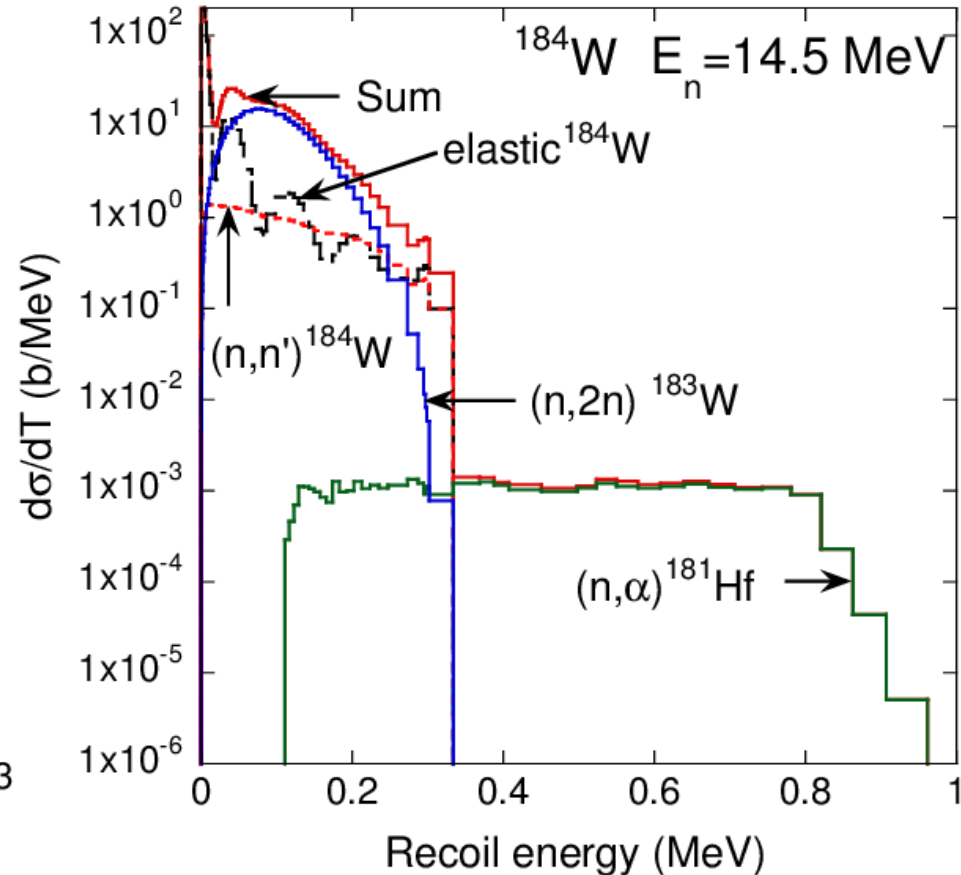
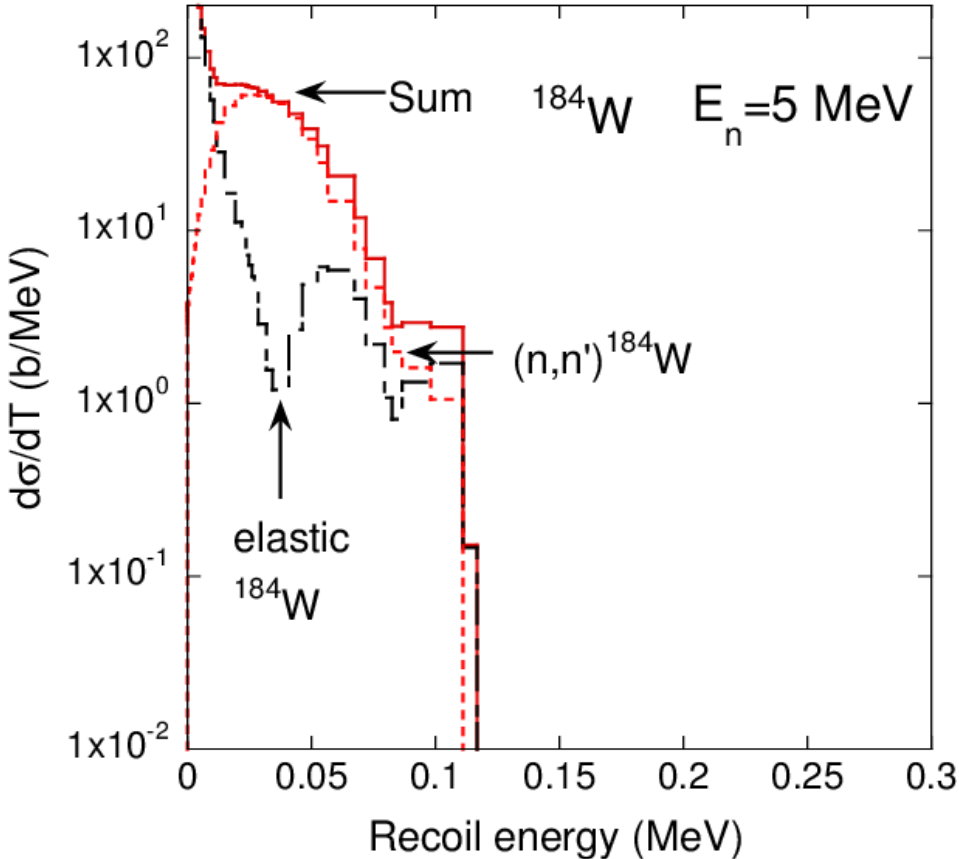
It is important to compare of PKA for each channel between codes.

PKA spectra for n+W



PKA spectra for n+W

Contribution of reaction channel to total using PHITS-EG-JENDL4.



5MeV: Contribution of elastic and (n,n') on PKA spectra are large.

14.5MeV: Contribution of $(n,2n)$ is also large. (n,α) is dominant for higher energy.

Comparison of PKA for each channel between codes will be needed.

Summary for PKA calculation

Calculation of PKA spectra on ^{28}Si , ^{56}Fe , ^{90}Zr and ^{184}W for 5 and 14.5 MeV neutrons.

For ^{28}Si and ^{56}Fe , good agreements between PHITS-EG and SPKA-END/F-BVII.1.

For ^{90}Zr and ^{184}W , SPKA-ENDF/B-VII.1 may lack some reactions.

Future plans:

- ✓ Calculation of PKA spectra at different radiation environments.
- ✓ Intecomparison of PHITS results with others.

Next slide: calculations of neutron kerma factors

(2) Calculations of neutron kerma factors

Neutron kerma : the sum of the initial kinetic energies of all the charged particles induced by neutron irradiation.

$$H(E) = \sum_i \sum_j \rho_i k_{ij}(E) \varphi(E) \longrightarrow \text{Neutron fluence}$$

Number density of material i

Neutron kerma factor
of material i , reaction j

$$k_{ij}(E) = \sum_l \bar{E}_{ijl}(E) \sigma_{ij}(E) \longrightarrow \text{Total neutron cross section}$$

Kinetic energy of secondary charged particle l : Heating number

- Heating number is obtained by NJOY and nuclear data.
- Heating numbers are included in the ACE file of data library.

Problem of neutron kerma factor in ACE file

- Energy balance method

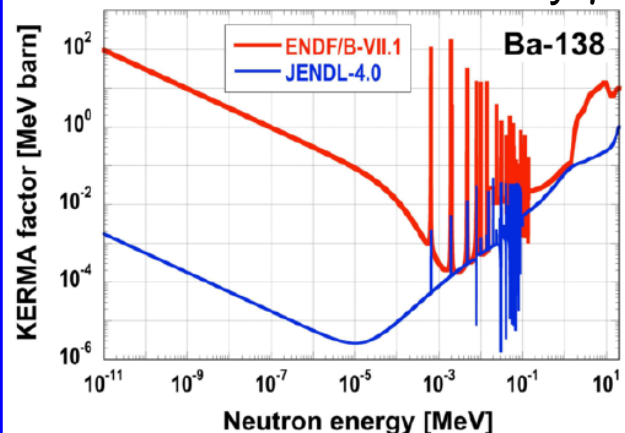
$$k_{ij}(E) = \left(\underset{\substack{\downarrow \\ \text{Incident neutron energy}}}{E} + Q_{ij} - \underset{\substack{\downarrow \\ \text{Total energy of secondary neutrons}}}{\bar{E}_{ijn}} - \overset{\substack{\rightarrow \\ \text{Total energy of secondary gamma rays}}}{\bar{E}_{ij\gamma}} \right) \sigma_{ij}(E)$$

- Kinematic method

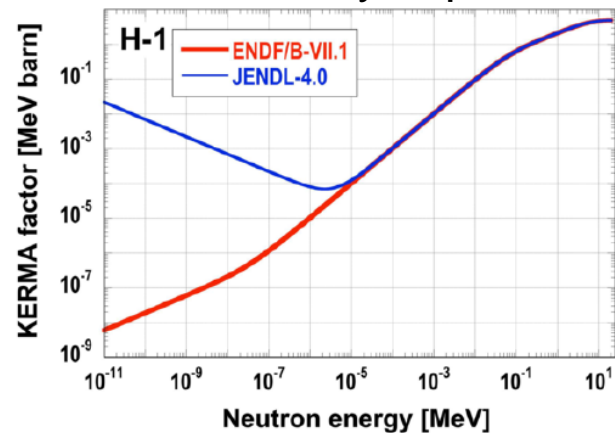
Calculation of upper limit of energy for charged particles.

Official ACE files { **END/F-BVII.1**: no check by Kinematic method
JENDL4: check by Kinematic method

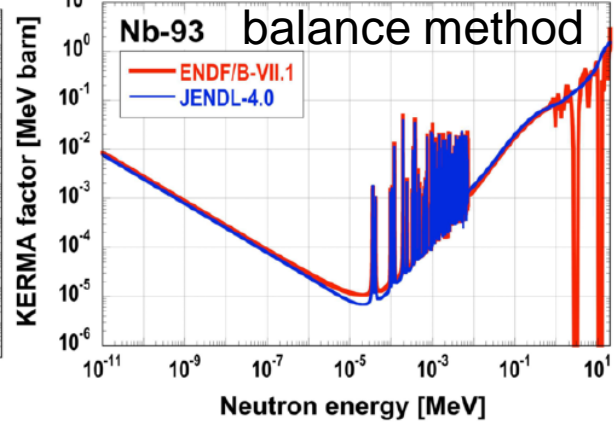
▪ no data for secondary γ



▪ no recoil by capture



▪ error in energy



More than 200 nucleus have problem for ACE files of END/F-BVII.1

Konno et al., Nuclear data sheet, 118 (2014) 450-452.

Necessary to validate kerma factors using new method

Purpose for kerma calculation

- Calculation of neutron heating number using **PHITS-EG**
- Comparison with data in ACE files and experimental data

Neutron energy range: 10^{-10} MeV \sim 20 MeV

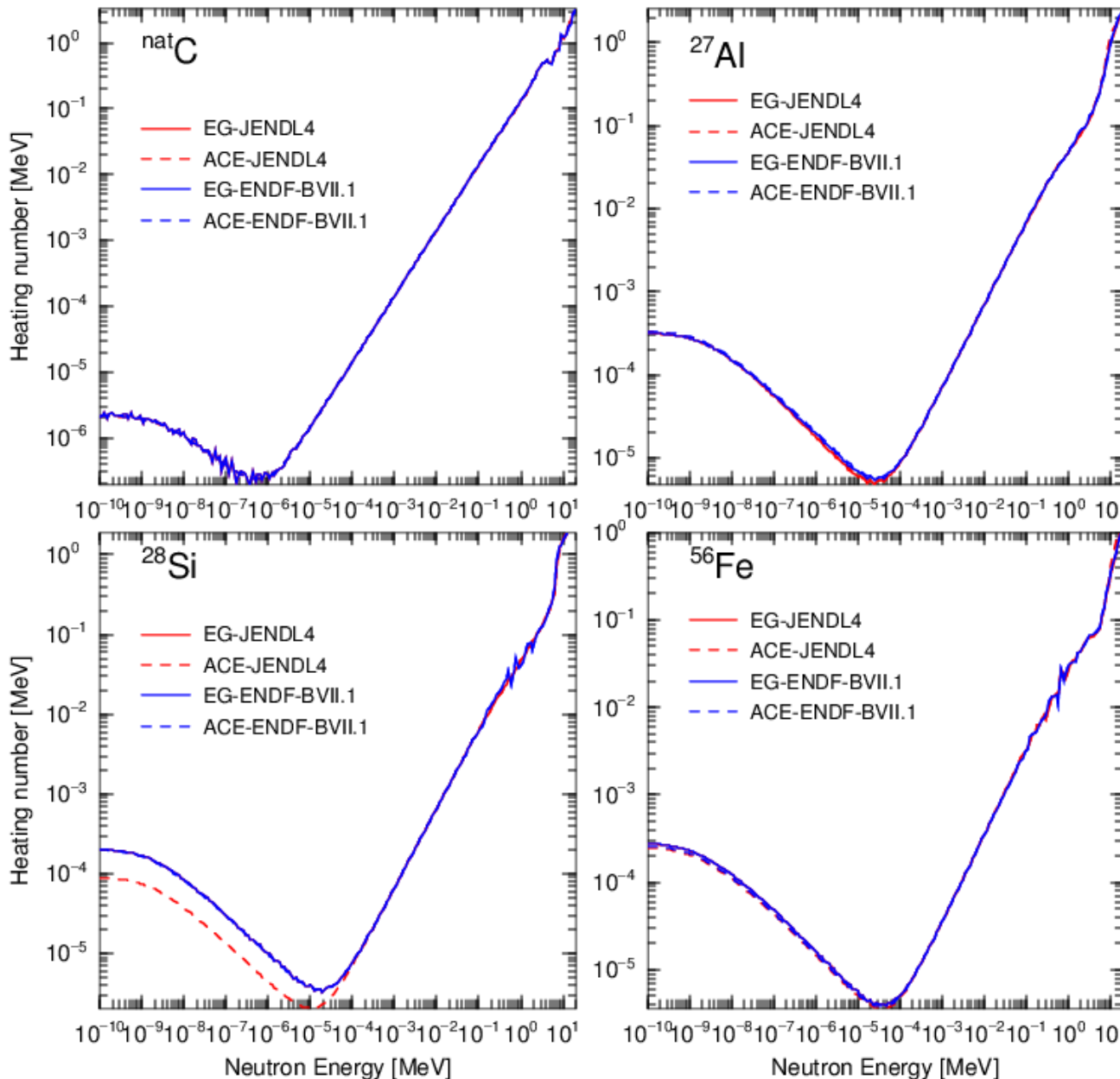
Elements of human body:

^1H , $^{\text{nat}}\text{C}$, ^{14}N , ^{16}O , ^{23}Na , ^{31}P , ^{32}S , ^{34}S , ^{35}Cl , ^{39}K , ^{41}K , ^{40}Ca

Structural materials:

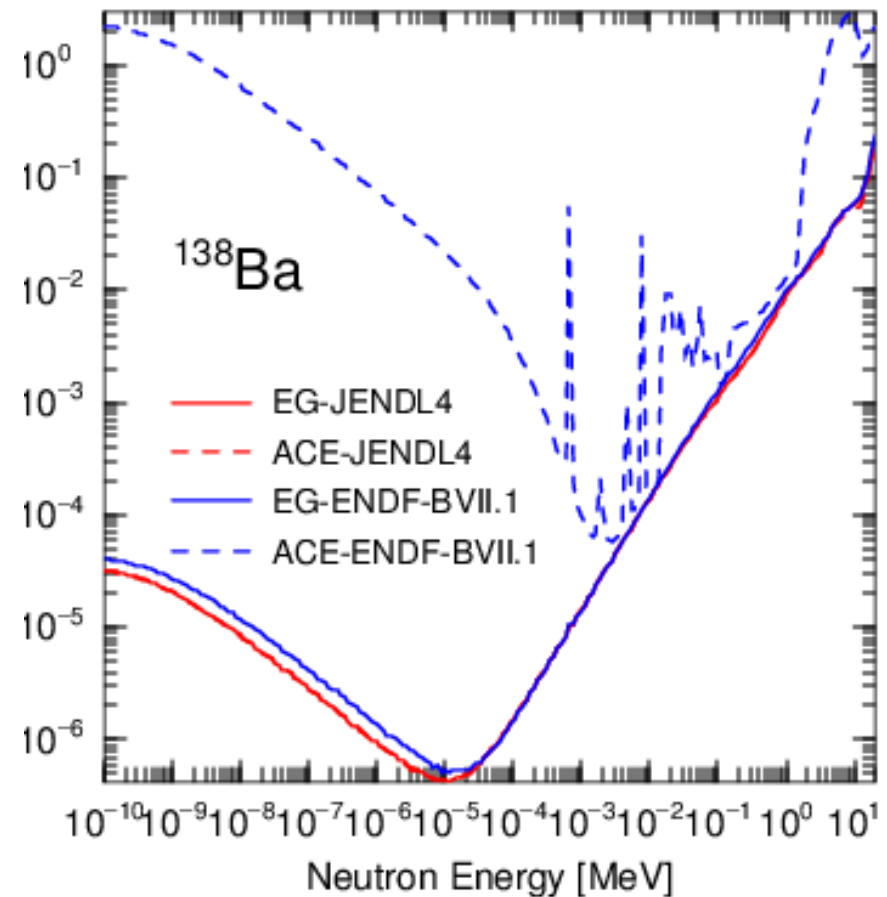
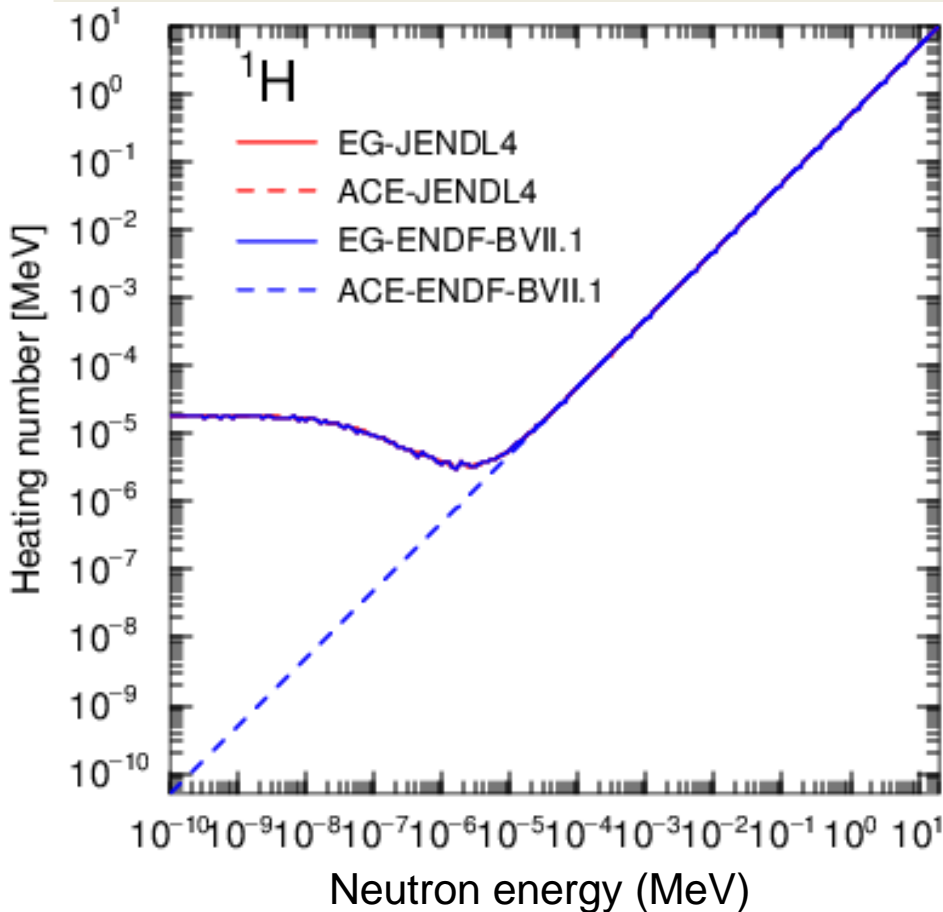
^{24}Mg , ^{27}Al , ^{28}Si , ^{56}Fe , ^{58}Ni , ^{63}Cu , ^{90}Zr , ^{138}Ba , ^{184}W , ^{208}Pb

Comparison of calculated results with values in ACE files



natC, ^{27}Al , ^{28}Si , ^{56}Fe :
Good agreements

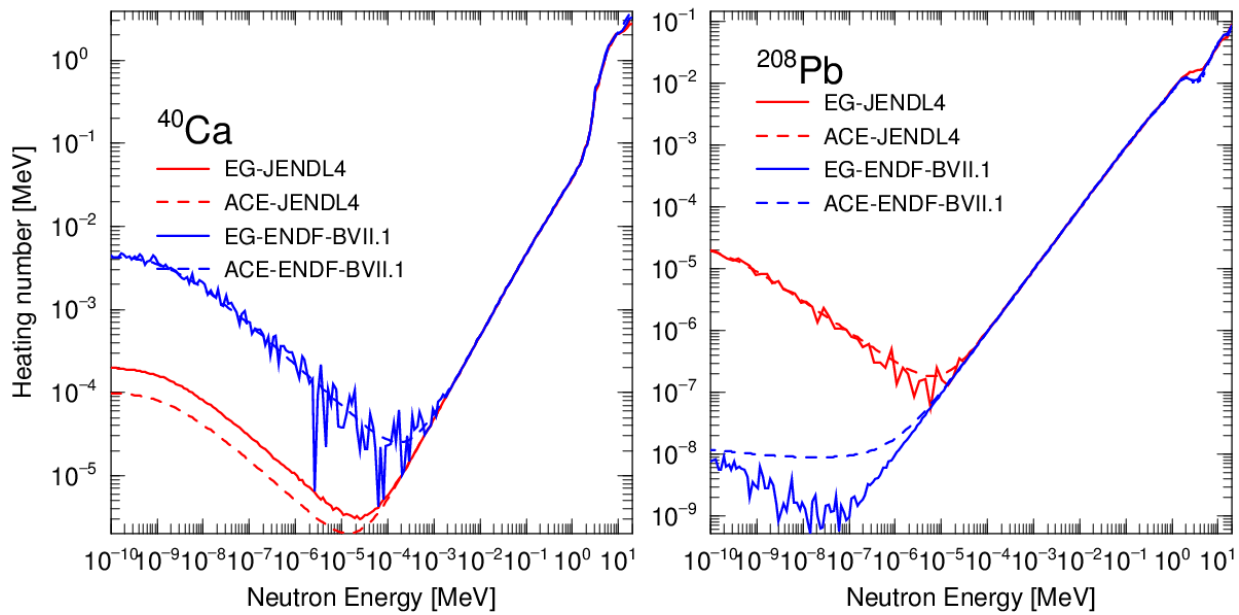
Comparison of calculated results with values in ACE files



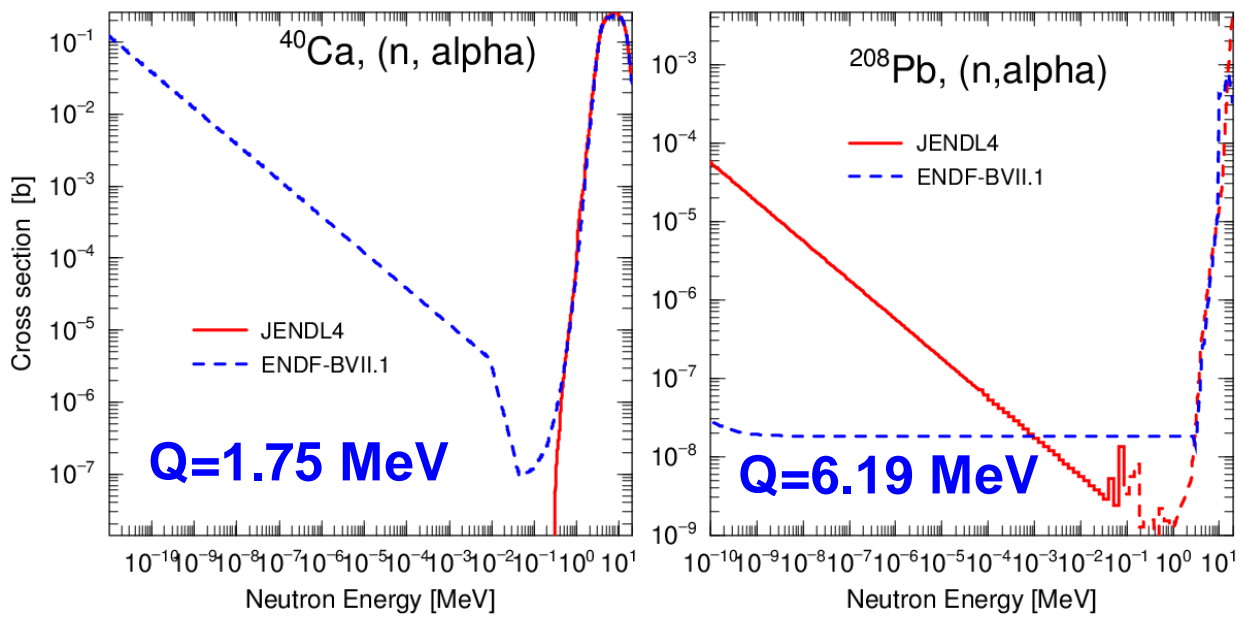
✓ PHITS-EG does not give strange results.

✓ PHITS-EG results are good agreements with value in ACE file of JENDL4.

Effects on Kerma due to difference of (n, α) cross section



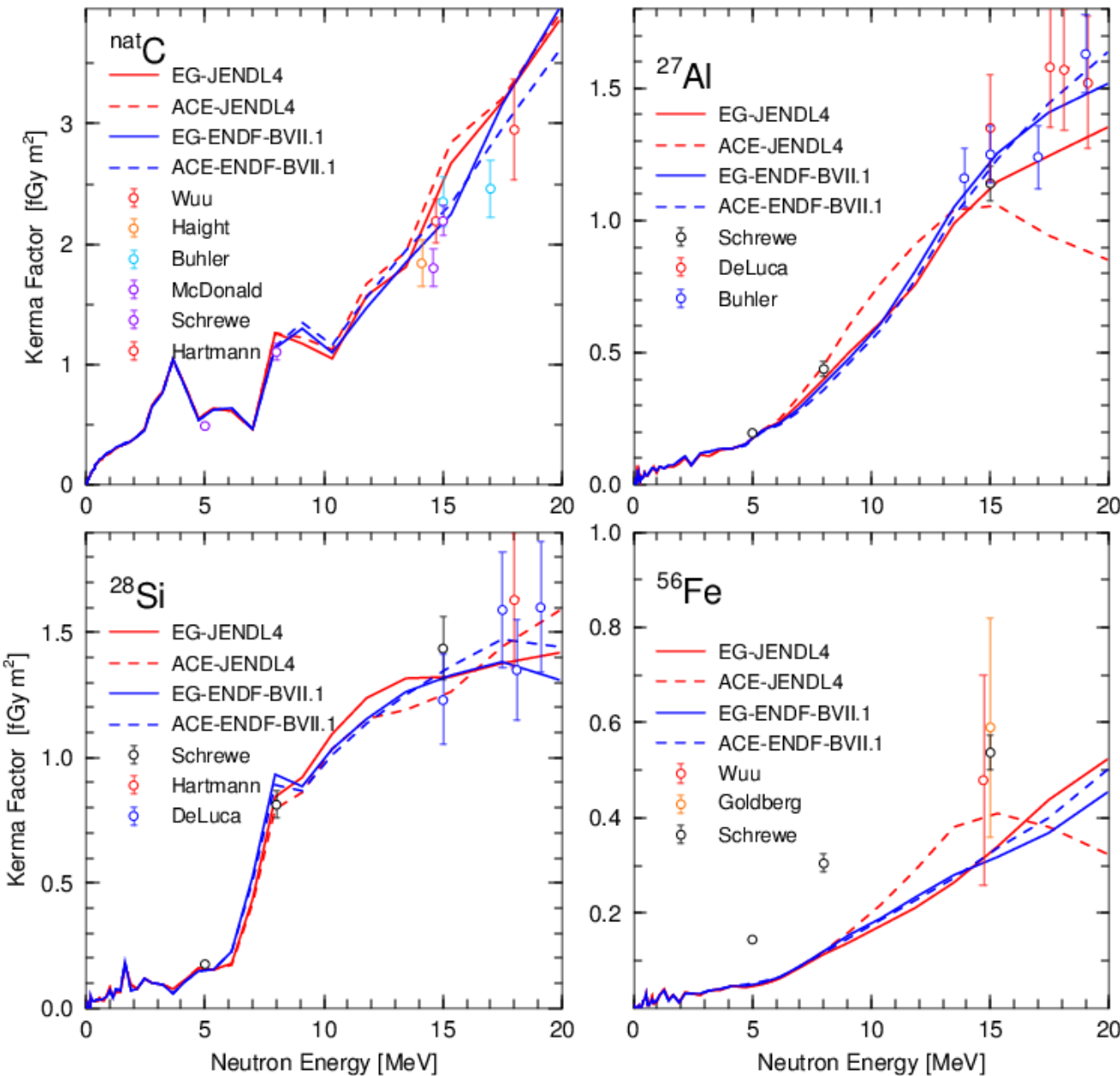
Large difference depending on nuclear data.



(n, α) cross section for JENDL4 is quite different from that for ENDF-BVII.1.

Necessary to re-evaluate (n, α) cross section.

Comparison with experimental data in high-energy region



natC, ²⁷Al, ²⁸Si: good agreements

⁵⁶Fe: underestimates

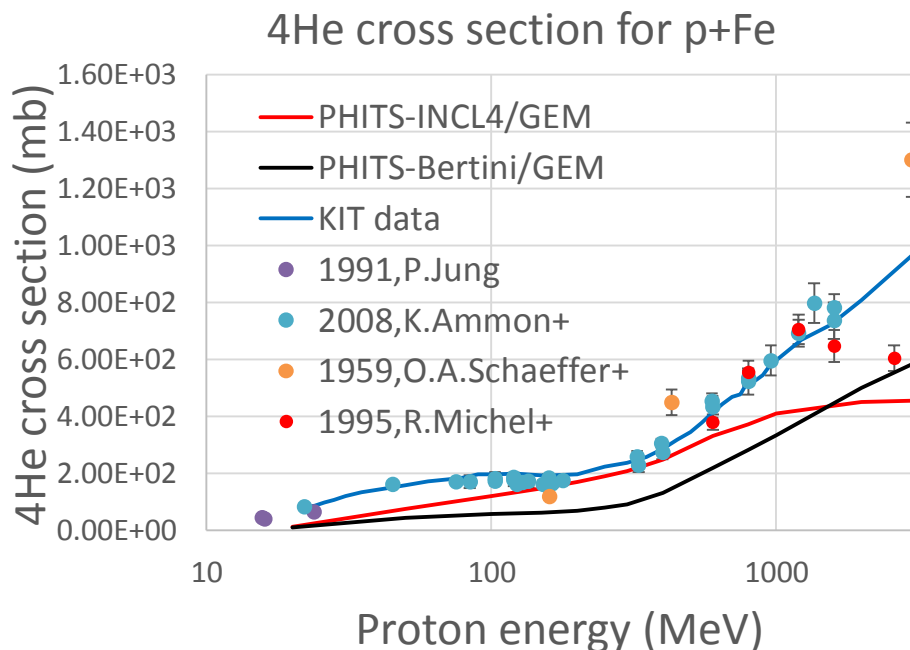
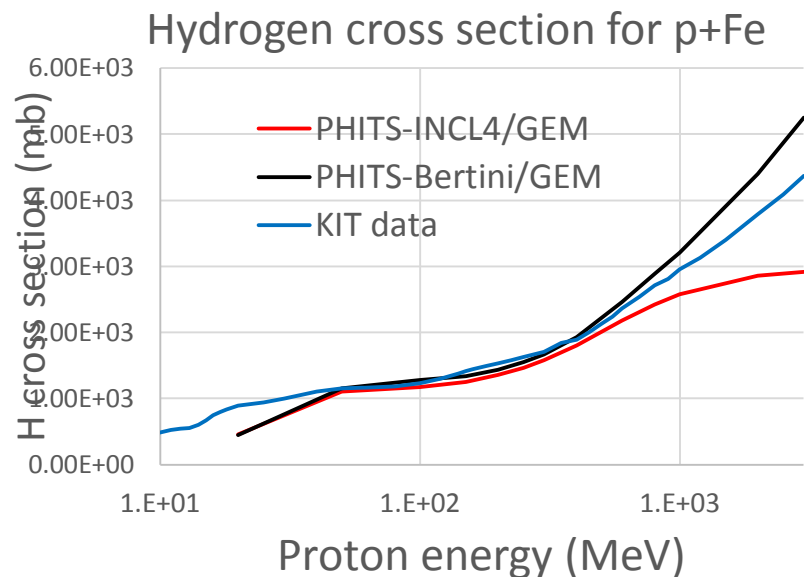
Summary for kerma calculations

- ✓ PHITS-EG does not introduce strange kerma factor obtained by the energy balance method.
- ✓ PHITS-EG generally agrees with values in ACE file.
- ✓ Neutron heating numbers for ^{40}Ca , ^{208}Pb are strongly depend on the (n,α) cross section in evaluated libraries.

Future plans : calculation and validation of kerma factors for heavier nuclei.

Next slide: calculations of gas production for p+Fe

(3) Intercomparison for gas production cross sections for p+Fe



KIT data: <https://www-nds.iaea.org/public/download-endf/DXS/>

Hydrogen: Good agreements with $80 \text{ MeV} < E_n < 500 \text{ MeV}$.

Helium: For INCL4/GEM, good agreements with $150 \text{ MeV} < E_n < 500 \text{ MeV}$.
For Bertini/GEM, generally underestimation.

Alpha particles are produced by evaporation process, mainly.

Applicable range of INCL/GEM is limited from 150MeV to 500MeV.

Future plans: calculation and validation for other materials

(4) Measurement of displacement cross section of copper irradiated with 125 MeV protons at 12 K

Y. Iwamoto^{*,a}, T. Yoshiie^b, M. Yoshida^c, T. Nakamoto^c,
M. Sakamoto^b, Y. Kuriyama^b, T. Uesugi^b, Y. Ishi^b, Q. Xu^b,
H. Yashima^b, F. Takahashi^a, Y. Mori^b, T. Ogitsu^c

^aJAEA ^bKURRI/Kyoto Univ. ^cKEK

Details are in [Journal of Nuclear Materials 458 \(2015\) 369–375](#).

Supported by a Japan Grant-in-Aid for Young Scientists (B) (25820450)
and “Clarification of material behaviors in accelerator driven systems by an FFAG
accelerator” carried out under the Strategic Promotion Program for Basic Nuclear Research
of the Ministry of Education, Culture, Sports, Science and Technology of Japan.

How to measure displacement cross section?

Irradiation on metal at cryogenic temperature

Recombination of Frenkel pairs by thermal motion is well suppressed.

Damage rate

$$\sigma_{\text{exp}} = \frac{1}{\rho_{FP}} \frac{\Delta\rho_{\text{metal}}}{\phi}$$

J. Nucl. Mater. 49 (1973/74) 161.

$\Delta\rho_{\text{metal}}$: Electrical resistivity change (Ωm)

Φ : Beam fluence ($1/\text{m}^2$)

ρ_{FP} : Frenkel-pair resistivity (Ωm)

Resistivity increase is the sum of resistivity per Frenkel pair

BNL data for 1.1 and 1.9 GeV: Cryostat assembly consisted of complicated system to deliver a flow of liquid cryogen.

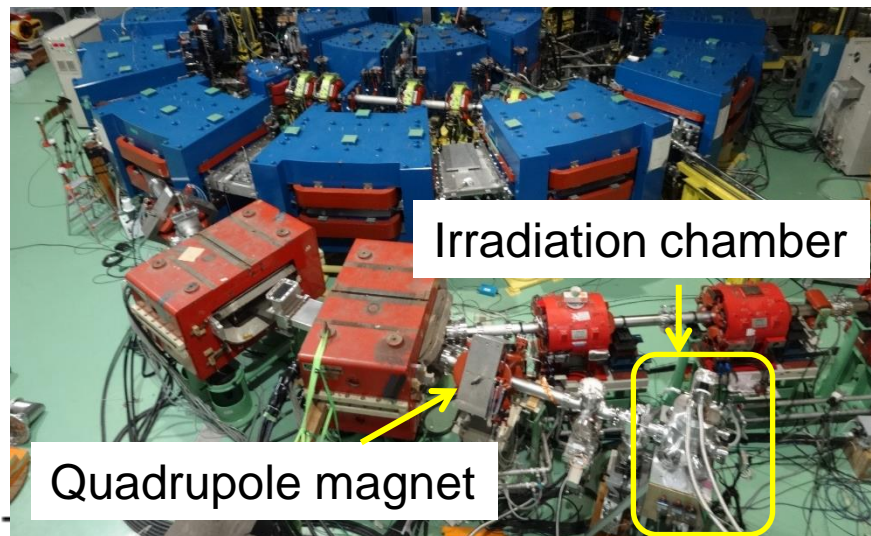
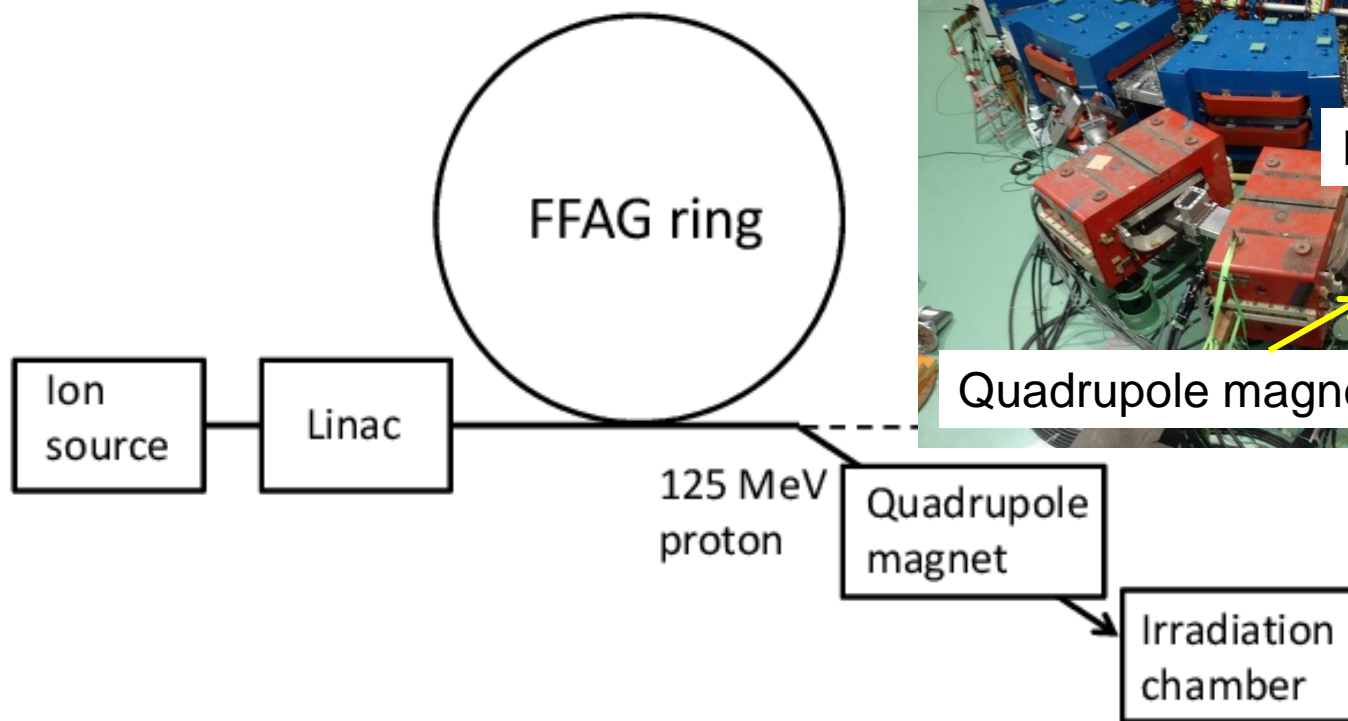
Hard to measure systematic data at other facilities with same device.

Development of cryogen-free cooling system

Measurements of damage rate of Cu under cryogenic irradiation

Beam line of FFAG accelerator facility

Fixed-Field Alternating Gradient (FFAG) accelerator facility at Kyoto University Research Reactor Institute (KURRI)



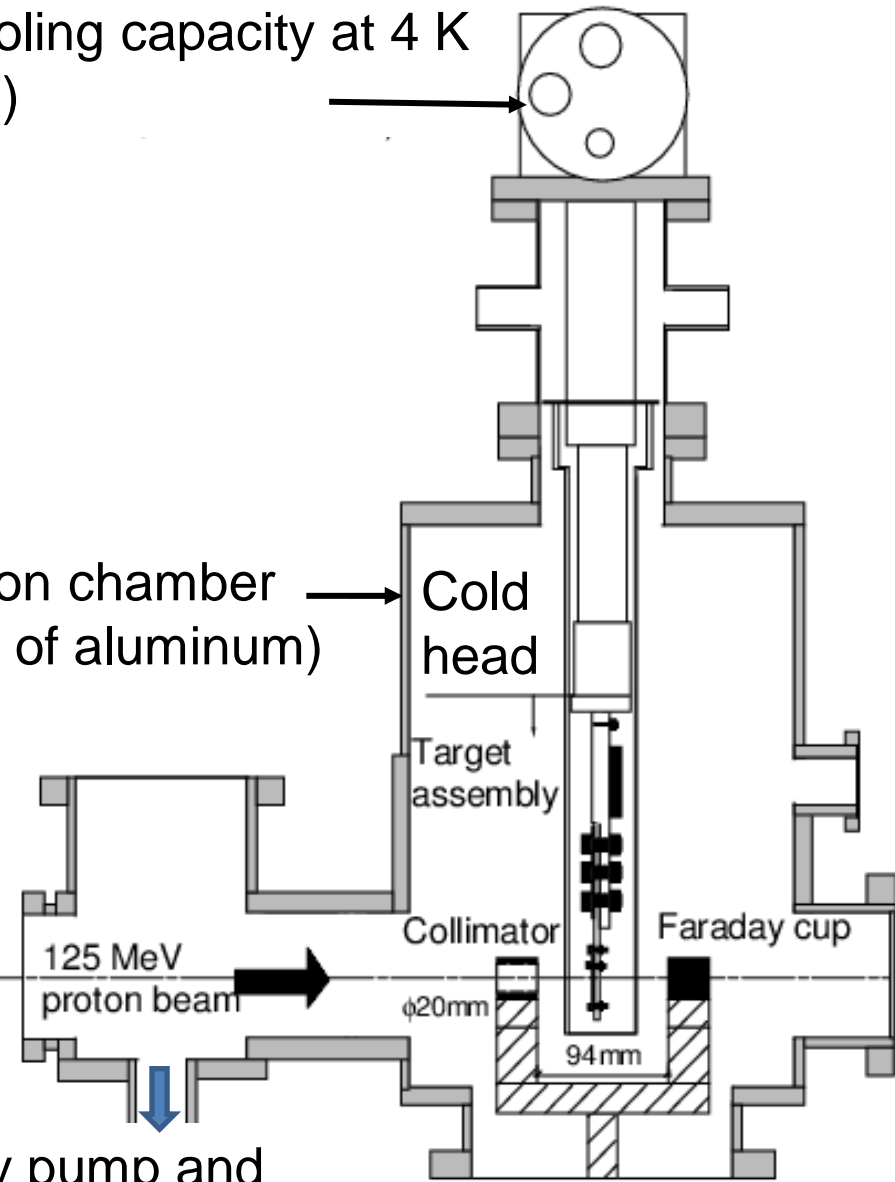
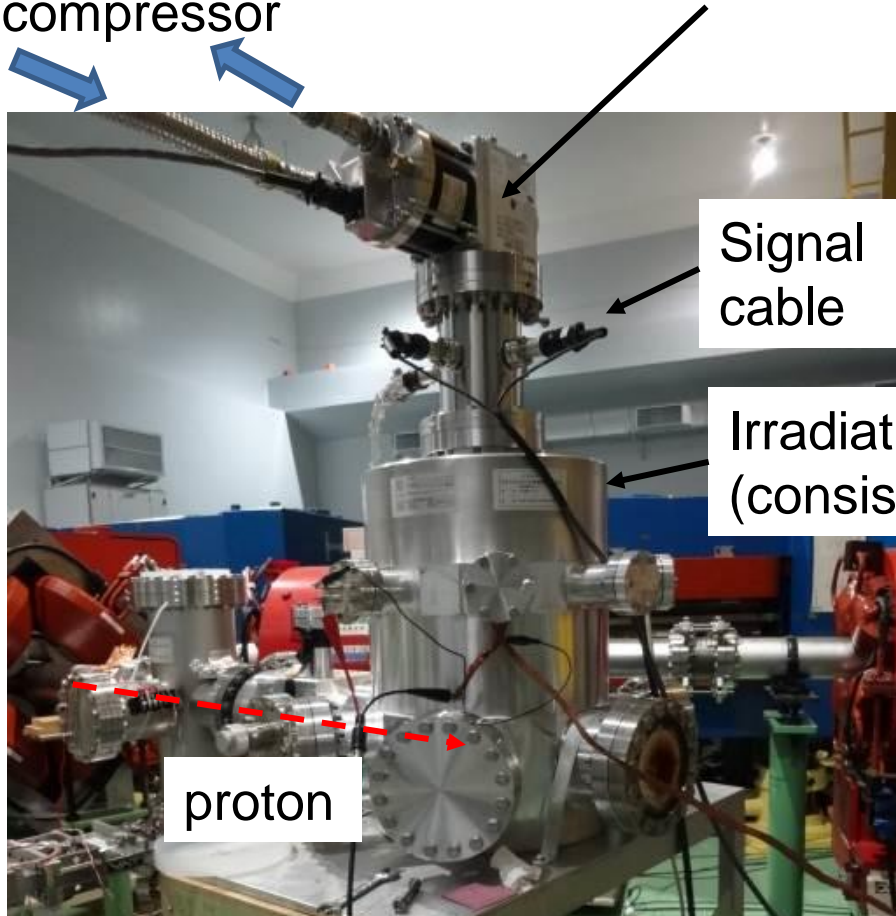
Proton energy: 125 MeV, 1 nA

Next slide: Irradiation chamber

Irradiation chamber with GM cryocooler

GM cryocooler 500 mW cooling capacity at 4 K

He gas lines (RDK-205E, Sumitomo inc.)
to compressor



Next slide: Target assembly

rotary pump and turbomolecular pump Vacuum of 10^{-5} Pa 27

Target assembly

✓ Sample was cooled by **conduction coolant** via Al (3) and oxygen-free high-conductivity copper (OFHC) (4).

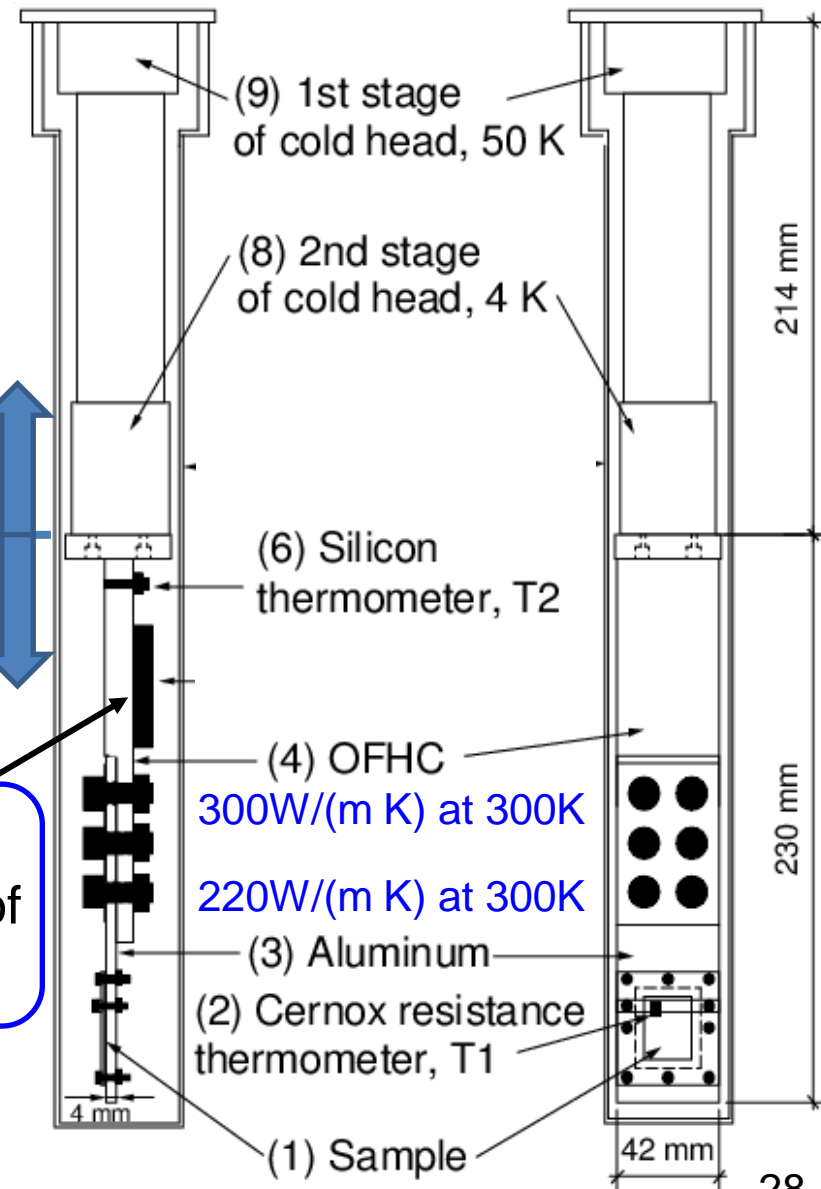


Cold head of GM cryocooler

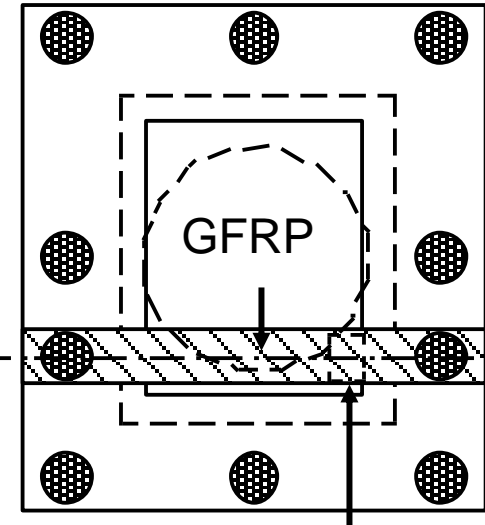
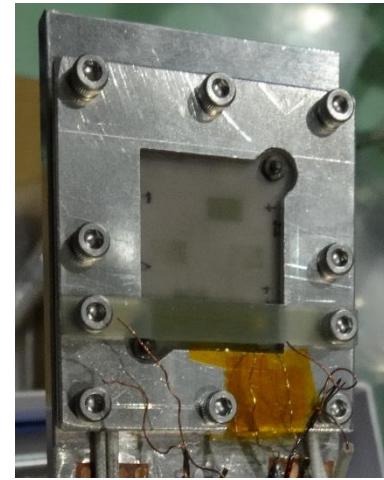
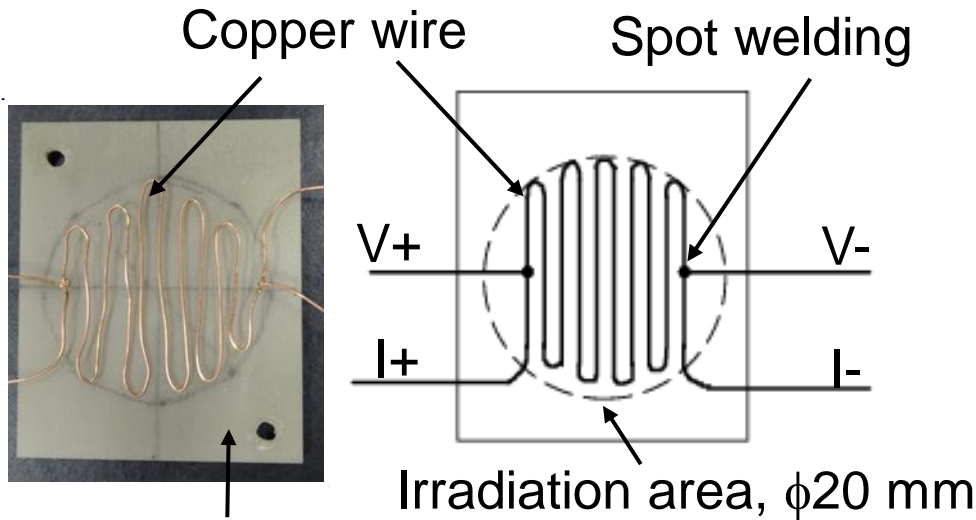
Target assembly

Electric heater:
Measurement of recovery of defects through annealing

Next slide: Sample



Sample and its retention

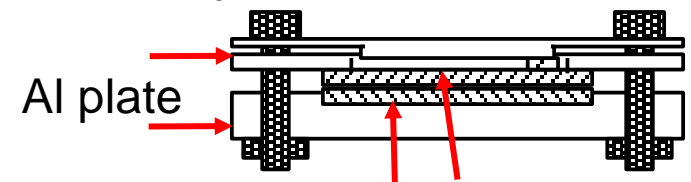


CX1050-SD Cernox
resistance thermometer

1.5-mm-thick AlN ceramic sheet

Electrical insulation and high thermal conductivity

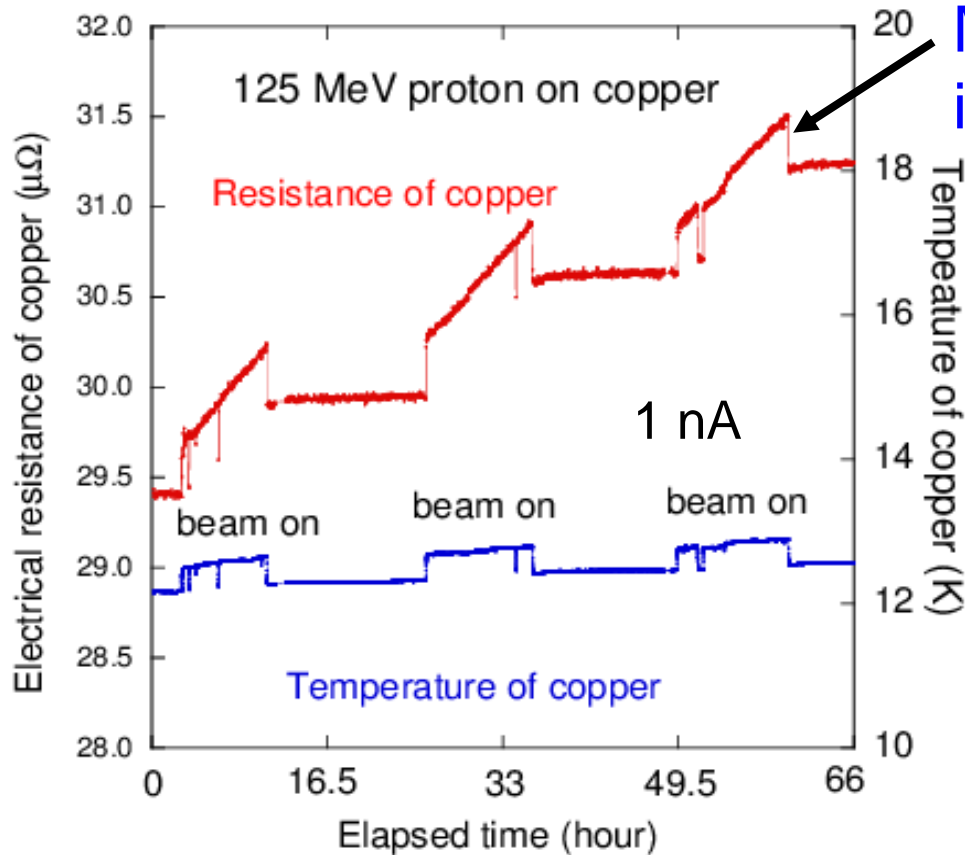
Material	Copper
Diameter (μm)	250
Purity (%)	99.999
Shape	a serpentine-shaped line Annealed for 1 h at 1000°C
Length between two potential points (mm)	152



Wire was carefully sandwiched between two 1.5-mm-thick AlN.

Next: Electrical resistance measurement

Electrical resistivity changes of copper during irradiation



Mainly resulted from temperature increase by beam heating.

Electrical resistance increase due to irradiation: $1.53 \mu\Omega$

ϕ (protons/m ²)	Resistivity increase $\Delta\rho_{\text{Cu}}$ ($\Omega \text{ m}$)	Damage rate ($\Omega \text{ m}^3/\text{proton}$)
1.45×10^{18}	4.94×10^{-13}	3.41×10^{-31}

Comparison with other experimental data

Source	Fast neutrons ANL-CP5- VI53 [1]	Fusion neutrons RTNS-II [2]	125 MeV protons KURRI-FFAG	1.94 GeV protons BNL [3]
Damage rate ($10^{-31} \Omega \text{ m}^3/\text{particle}$)	0.424	2.48	3.41	3.66

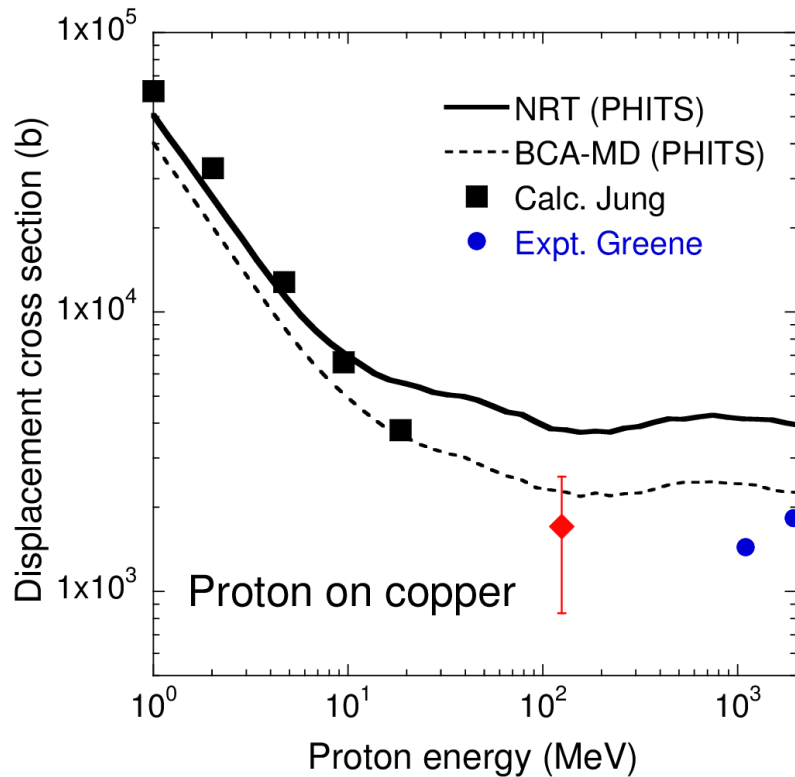
- ✓ The damage rates by neutrons increase with incident energies up to 14 MeV.
- ✓ Those by protons with energies >100 MeV are higher than the damage rate by 14 MeV neutrons.

[1] J.A. Horak, T.H. Blewitt, J. Nucl. Mater. 49 (1973/74) 161–180.

[2] M.W. Guinan, J.H. Kinney, J. Nucl. Mater. 108&109 (1982) 95–103.

[3] G.A. Greene, et al., Proceedings of AccApp'03, 2004, p.881–892.

Displacement cross section



Large difference between experimental data and NRT (no defect production efficiency)

The measured data agrees better with BCA-MD (defect production efficiency)

Main uncertainty comes from ρ_{FP} .

$$\sigma_{\text{exp}} = \frac{1}{\rho_{FP}} \frac{\Delta\rho_{\text{metal}}}{\phi}$$

Damage rate = $3.41 \Omega\text{m}^3$

↓ Resistivity change / Frenkel pair density

$2.0 \times 10^{-6} \Omega\text{m}$, 50 % uncertainty

P. Ehrhart, U. Schlagheck, J. Phys. F: Metal Phys. 4 (1974) 1575–1588.

Can be derived from damage rate measurements in single crystals under electron irradiation at low temperature

Summary for experimental study

Summary

Cryogenic irradiation system has been developed.

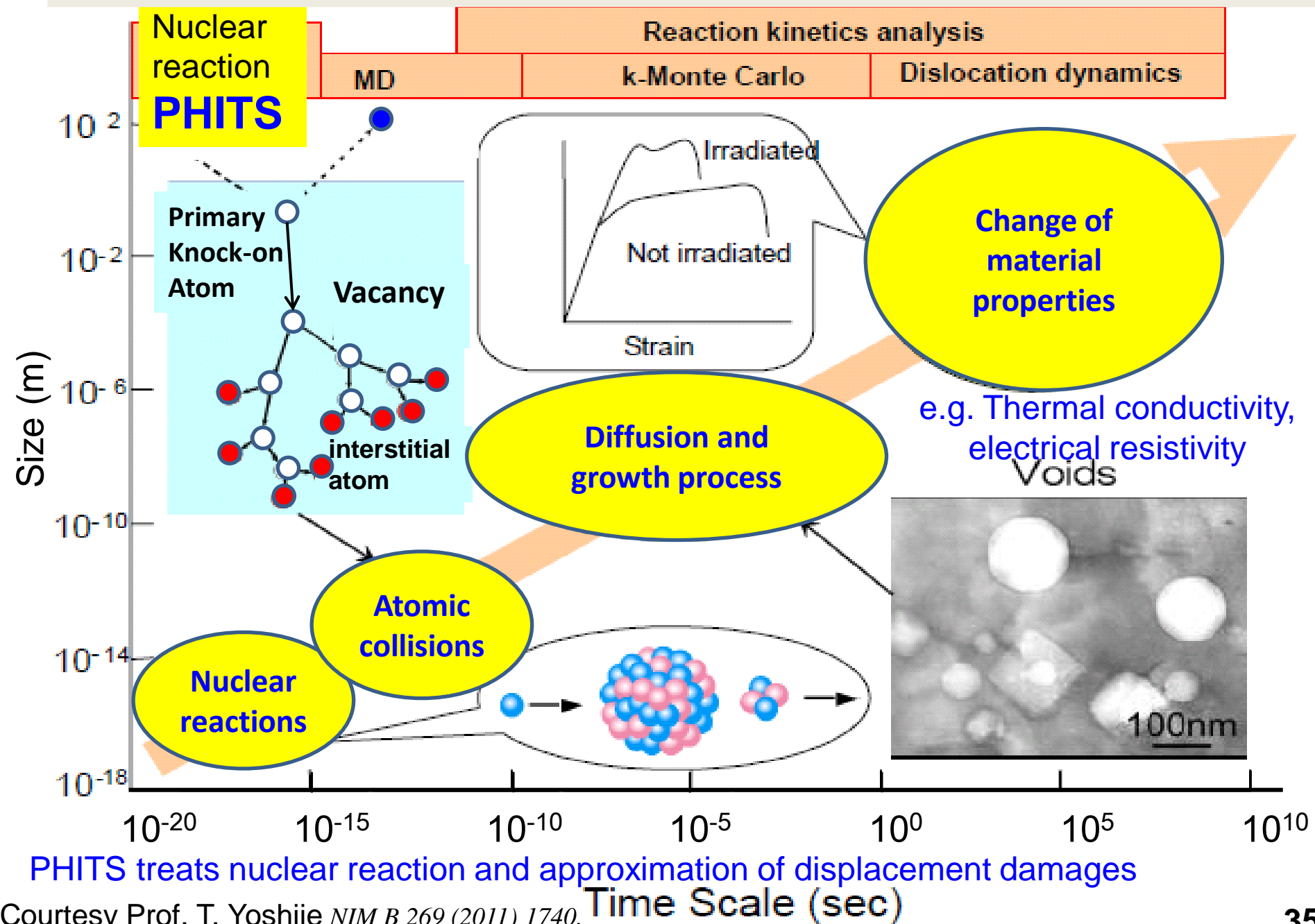
- Sample was cooled by conduction coolant via Al and OFHC.
- σ_{BCA-MD} is in better agreement with experimental data than σ_{NRT} .
But, it still overestimates the experimental data.

Future plans

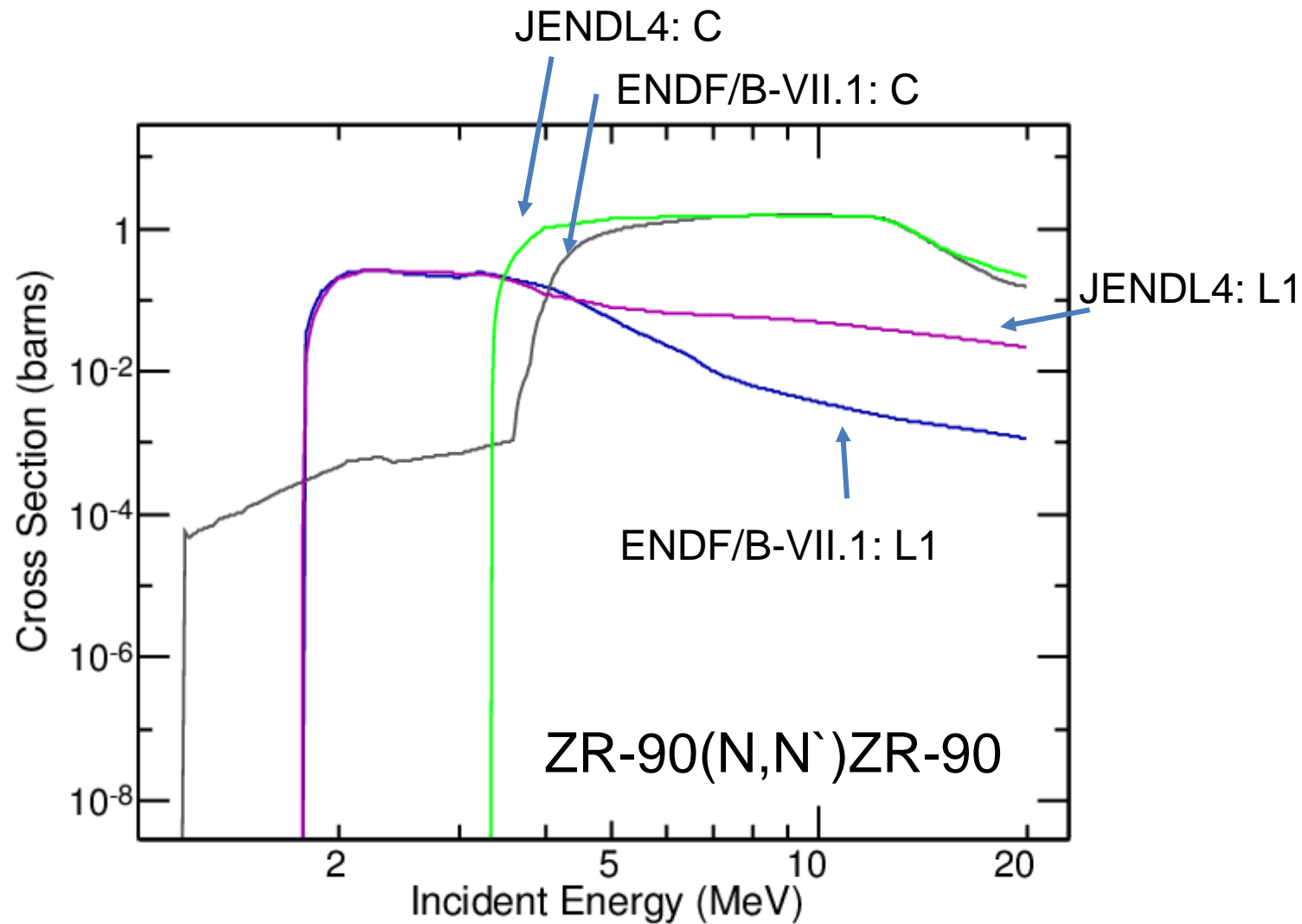
- Improving cooling system.
- Measurements under 125 MeV proton on Al at KURRI.
- Move the device to other facilities, such as RCNP and FNAL.
- Measurements for 100 MeV - 100 GeV proton on metals.

Thank you for your attention.

Scale of irradiation effect



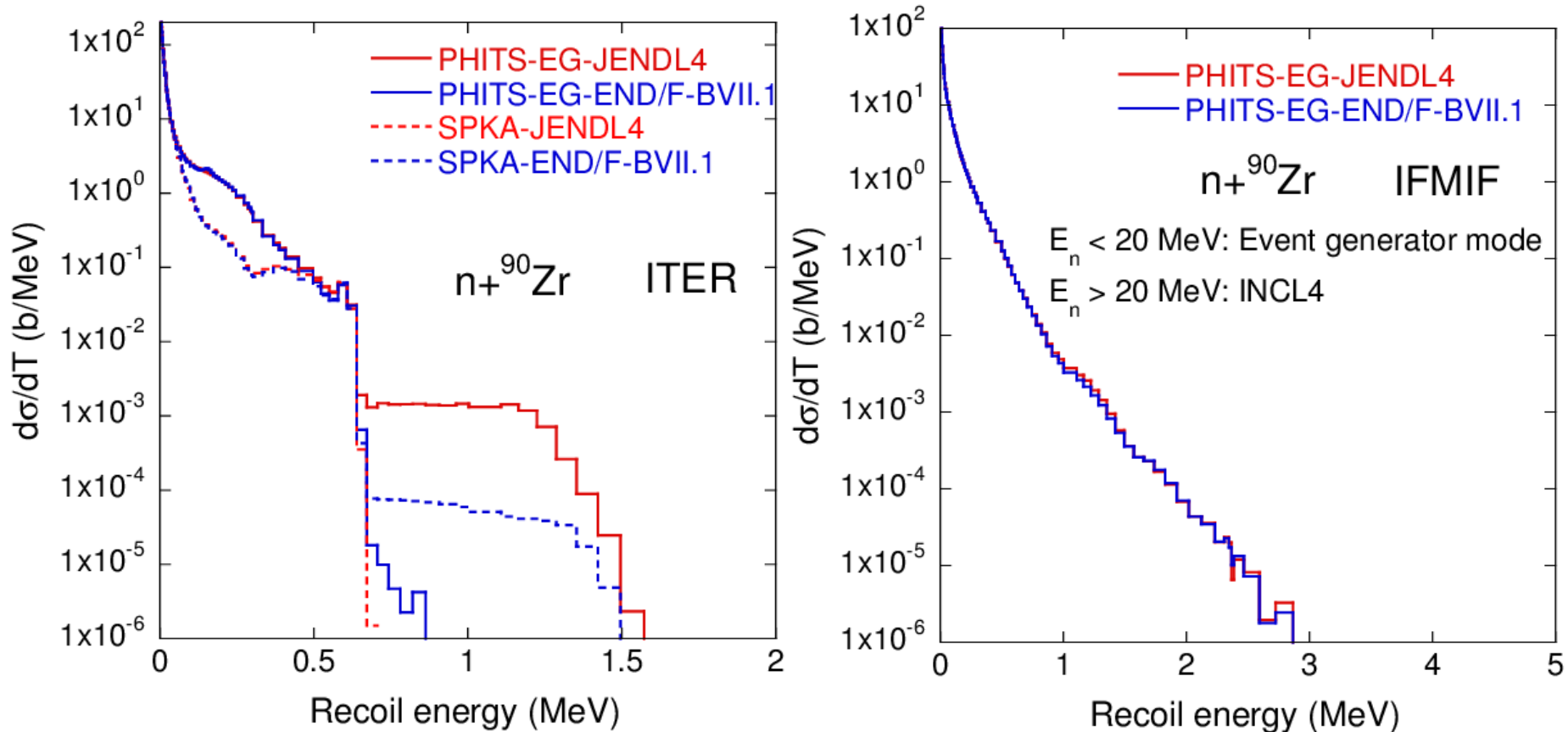
PHITS treats nuclear reaction and approximation of displacement damages



C: Production of a neutron in the continuum not included in the discrete represent.

L1: Production of a neutron, with residual in the 1st excited state.

PKA spectra for ^{90}Zr at ITER and IFMIF

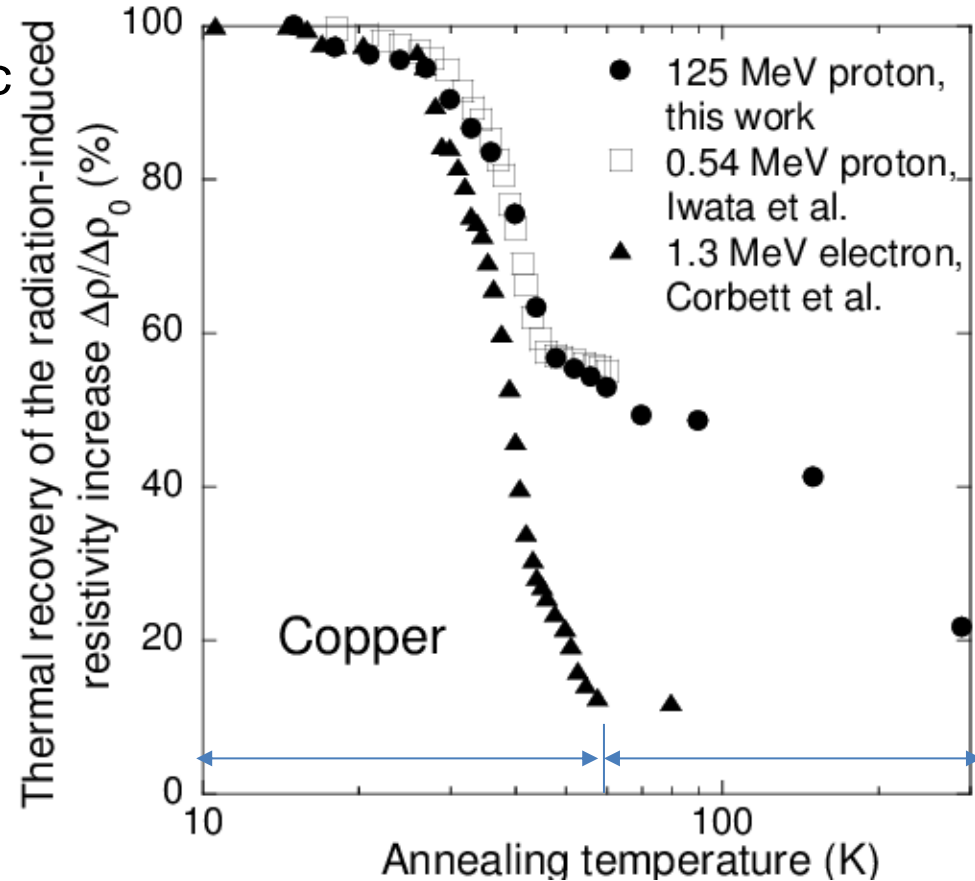


SPKA-ENDF/B-VII.1 is close to SPKA-JENDL4 below 0.6 MeV.

Recovery of defects through annealing after irradiation

Annealing effects up to certain temperatures were observed using isochronal schedule.

- (1) Warming the sample by the electric heater at annealing temperature.
- (2) Holding the temperature of the sample constant for 10 min.
- (3) Cooling the sample to 12 K.
- (4) Measuring the electric resistivity of the sample at 12 K.

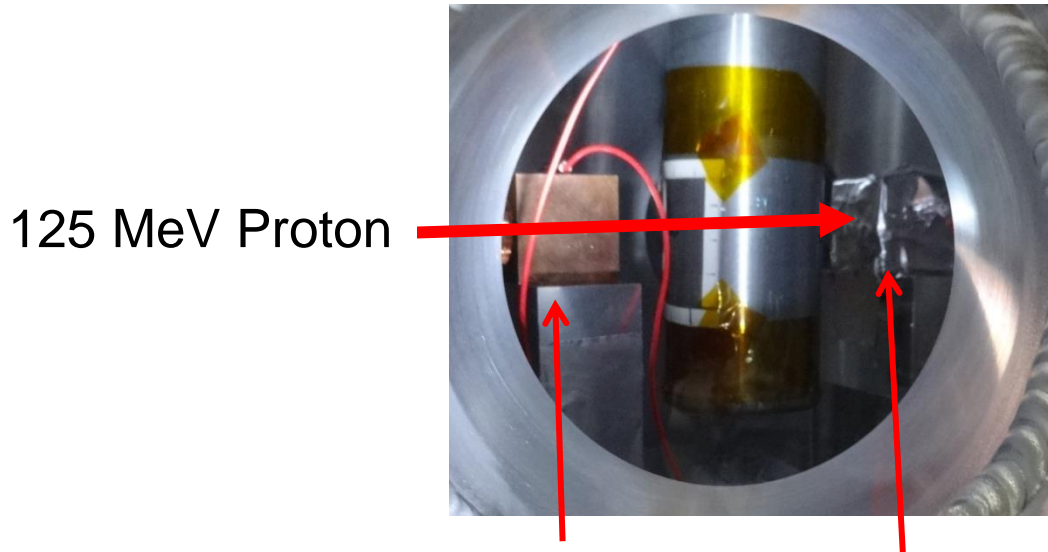


Behavior of resistivity recovery for 125 MeV is similar to that for 0.54 MeV.

Essentially no damage was recovered below 15 K, where Frenkel defects were almost immobile.

How to measure beam fluence(protons/m²) ?

The number of protons on the sample during irradiation was measured in situ by the Faraday cup.



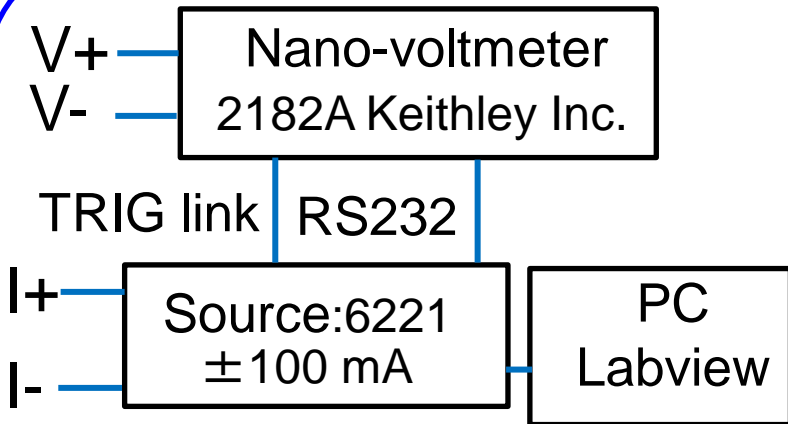
Copper collimator with $\phi 2$ cm hole

Faraday cup, 3 cm thick Cu block

- ✓ Reduce halo of proton striking the thermometer on the sample.
- ✓ Cu block was insulated by Kapton polyimide tape to ensure secondary electrons do not escape from Cu block.

An **activation measurement** was carried out .

Electrical resistance of copper wire

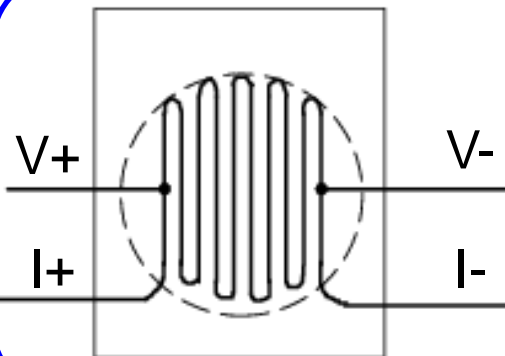


A current of ± 100 mA was fed into copper wire with polarity changing at a frequency of 10 Hz.



Cancel effects of thermal electromotive force

Precision of this resistance measurement was $\pm 0.01 \mu\Omega$,
Corresponding to a resistivity of $\pm 3 \text{ f}\Omega \text{ m}$.



Electrical resistivity

$$\rho_{Cu} = R A / L$$

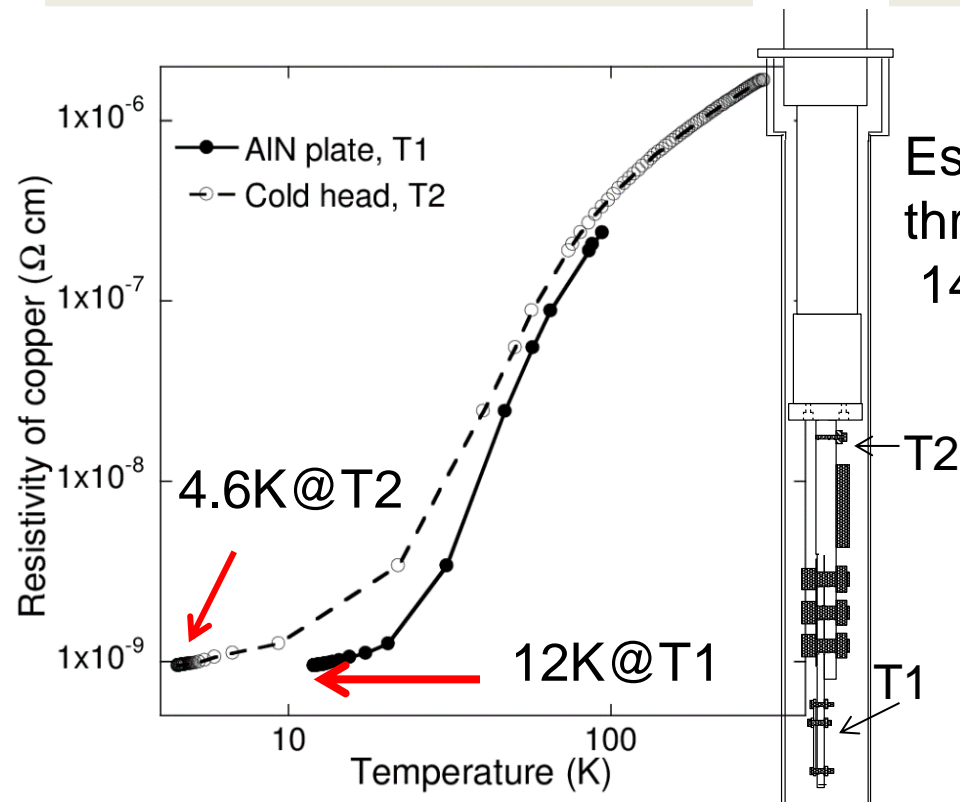
R: Measured electrical resistance

L: Length between two potential points (152 mm fixed)

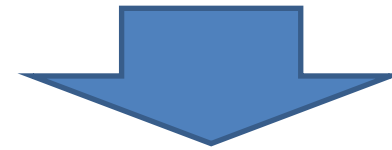
A: Area of the sample ($4.91 \times 10^{-2} \text{ mm}^2$ fixed).

Next: Cooling test

Cooling test for sample



Estimated heat entering the sample through signal cable and thermal radiation 14 mW: much less than 500 mW power .



• Insufficient thermal contact between the aluminum columns and AlN sheets.

Material	Copper
Resistivity at 298 K ($\Omega \text{ m}$)	1.67×10^{-8} (52.0 m Ω)
Resistivity at 12 K ($\Omega \text{ m}$)	9.44×10^{-12} (29.4 $\mu\Omega$)
Residual resistivity ratio (RRR)	1769

Next slide: How to measure beam fluence on sample

Why is damage rate important?

The average number of displaced atoms per atom of a material

$$\mathbf{DPA} \text{ (displacement per atom)} = \int \sigma_{\text{disp.}}(E) \phi(E) dE$$

Displacement cross section

Calculation

$$\sigma_{\text{calc.}} = \sum_i \int_{E_d}^{T_i^{\text{max}}} d\sigma/dT_i \times v(T_i) dT_i$$

$d\sigma/dT_i$: recoil atom energy distribution

$$v(T_i) = N_{\text{NRT}} = 0.8 T_{\text{dam}} / (2E_d)$$

$v(T_i)$: number of defects

T_{dam} : Damage energy

E_d : threshold displacement energy

$$\text{or } v(T_i) = \eta N_{\text{NRT}}$$



Defect production efficiency by MD-BCA

Measurement

Irradiation at cryogenic temperature

Recombination of Frenkel pairs by thermal motion is well suppressed.

$$\sigma_{\text{exp}} = \frac{1}{\rho_{\text{FP}}} \frac{\Delta\rho_{\text{metal}}}{\phi} \quad \text{Damage rate}$$

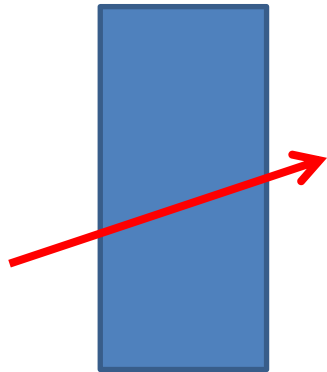
$\Delta\rho_{\text{metal}}$: Electrical resistivity change (Ωm)

Φ : Beam fluence ($1/\text{m}^2$)

ρ_{FP} : Frenkel-pair resistivity (Ωm)

J. Nucl. Mater. 49 (1973/74) 161.

PHITS simulation



Average energy E_{ave} of a charged particle in a region

(E_{ave}, M_1, Z_1)

To check the accuracy of calculation of PKA for each reaction channel, **Displacement cross section σ**
It is important to compare of PKA for each channel between codes.

e1

e2

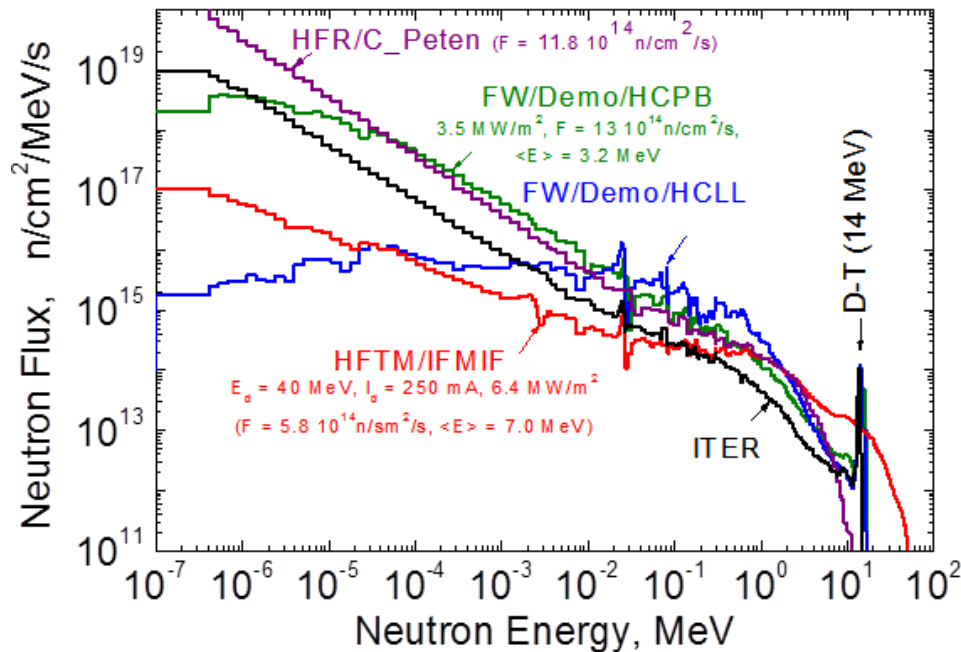
Range(e1)

Range(e2)

$Delt = Range(e1) - Range(e2)$

$$DPA = \frac{\sum (\sigma \times delt \times dens)}{\sum dens \times Volume}$$

(2) Calculation of PKA spectra using PHITS-EG and NJOY-SPKA for different radiation environments



Neutron source	Targets
Demo/HCLL	Fe, Zr, SiC
IFMIF	Fe, Zr, SiC
ITER	Fe, Zr, SiC

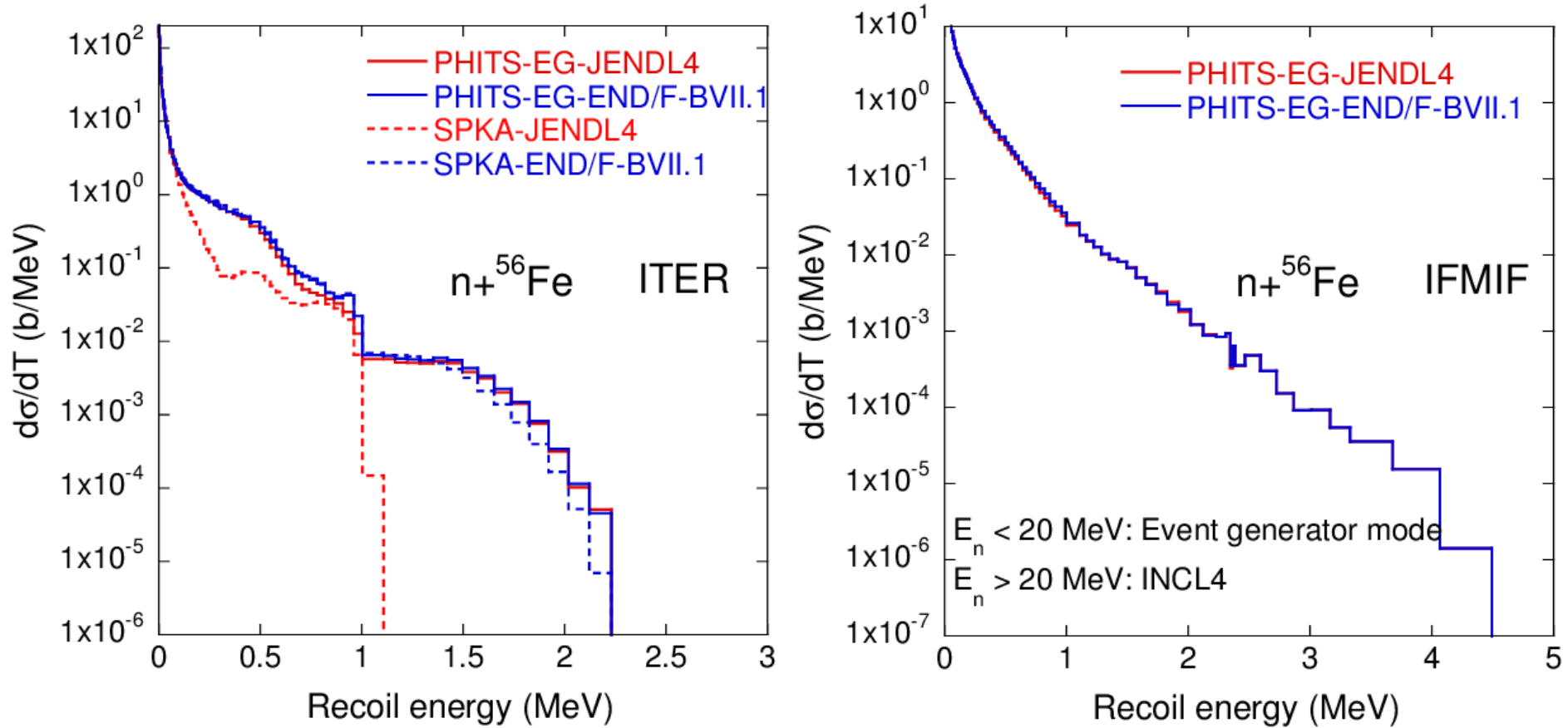
Processing step	Library
PHITS-EG	JENDL-4
PHITS-EG	ENDF/B-VII.1
NJOY-SPKA	JENDL-4
NJOY-SPKA	ENDF/B-VII.1

from <https://www-nds.iaea.org/CRPdpa/>

PHITS-EG: $E_n < 20 \text{ MeV}$ Event Generator mode
 $E_n > 20 \text{ MeV}$ INCL4 intra nuclear cascade model

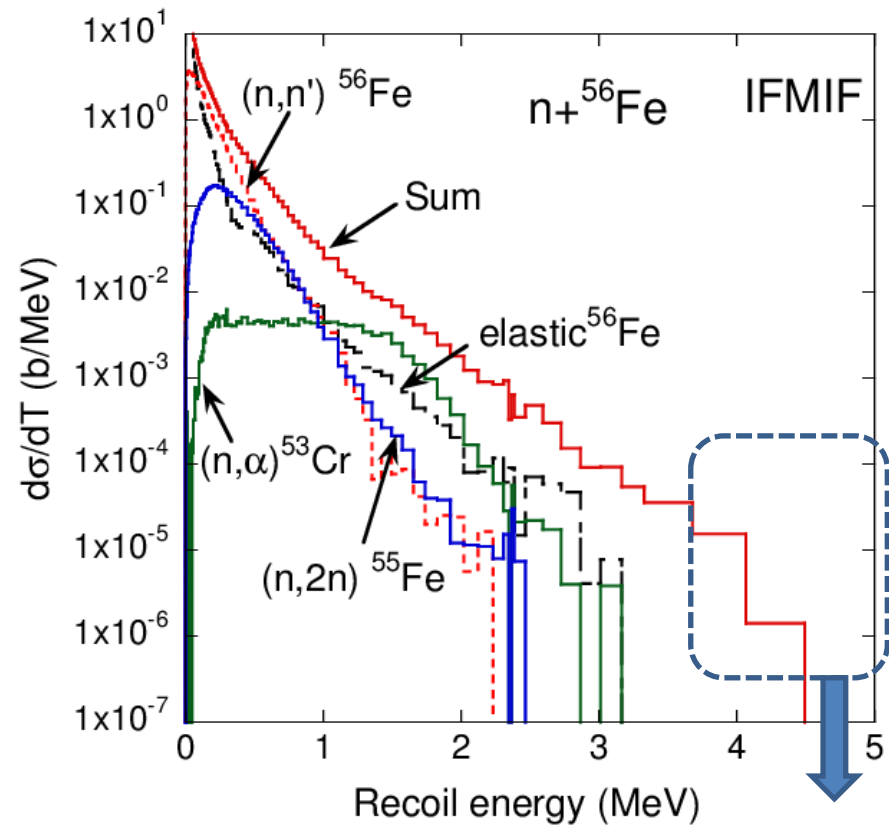
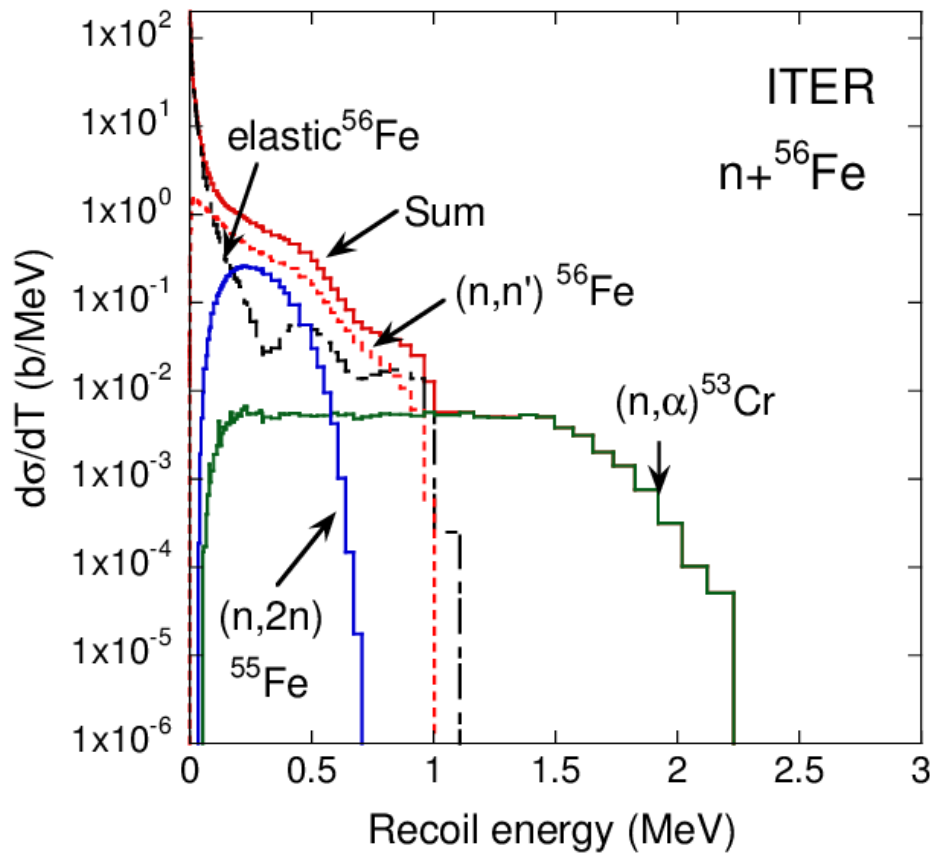
PKA group structure is [vitamin-j 175-group](#).

PKA spectra for $n+^{56}\text{Fe}$



Good agreements except for SPKA-JENDL4

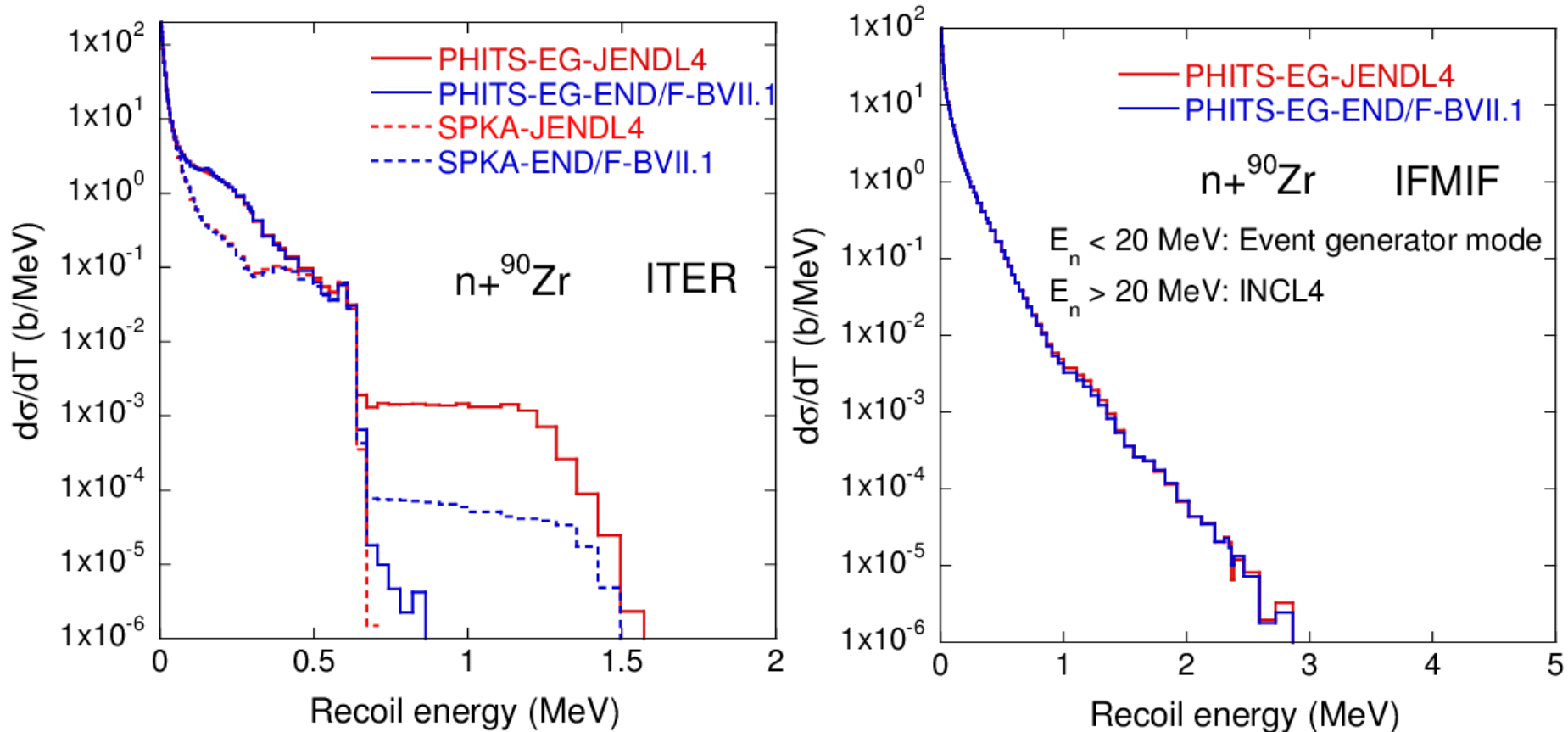
PKA spectra for $n+^{56}\text{Fe}$



51Cr, 52Cr, 51V from spallation reactions

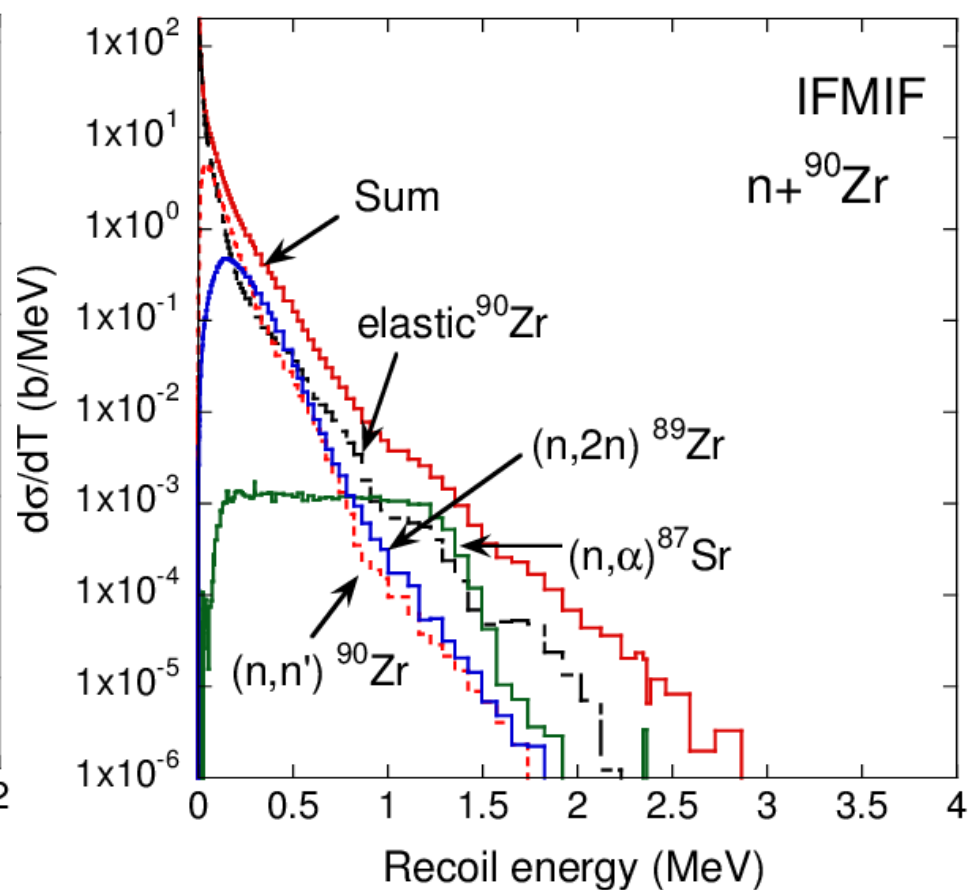
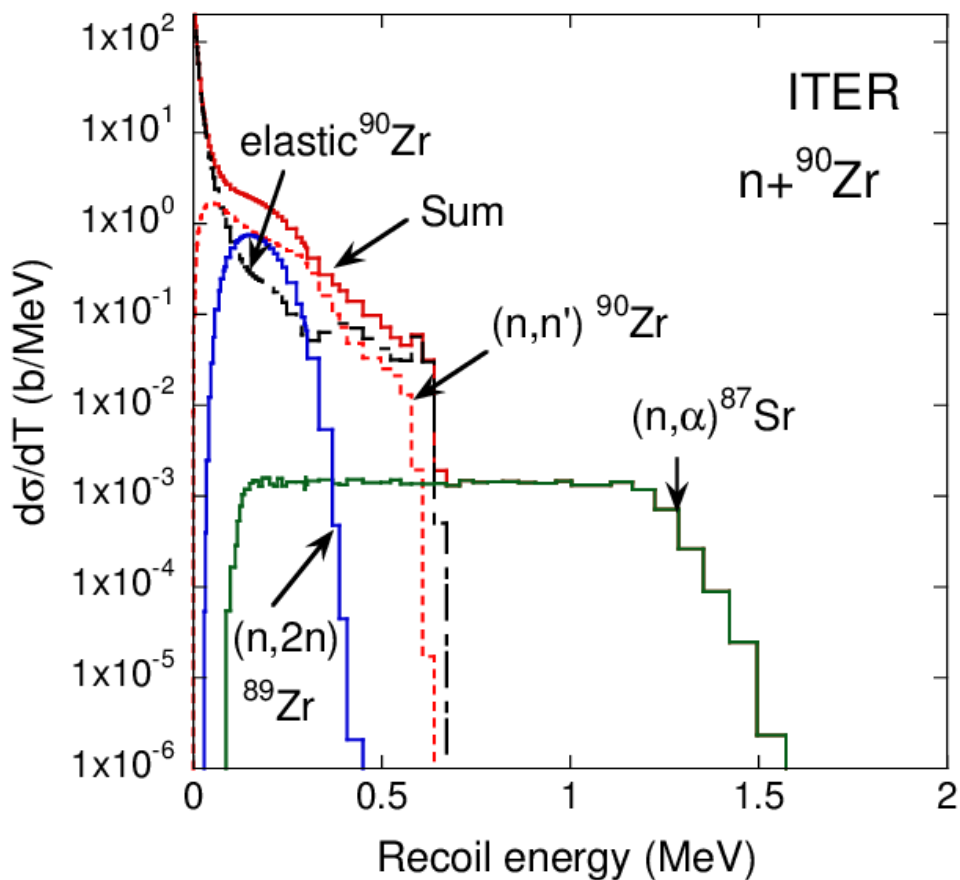
Good agreements except for SPKA-JENDL4

PKA spectra for $n+^{90}\text{Zr}$

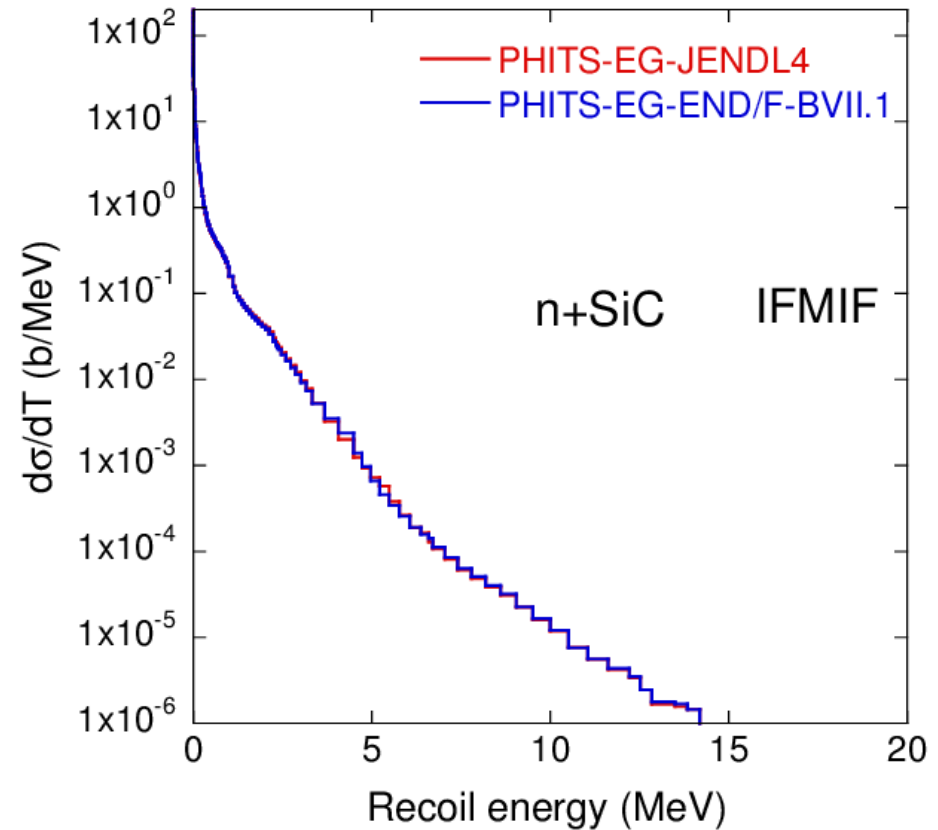
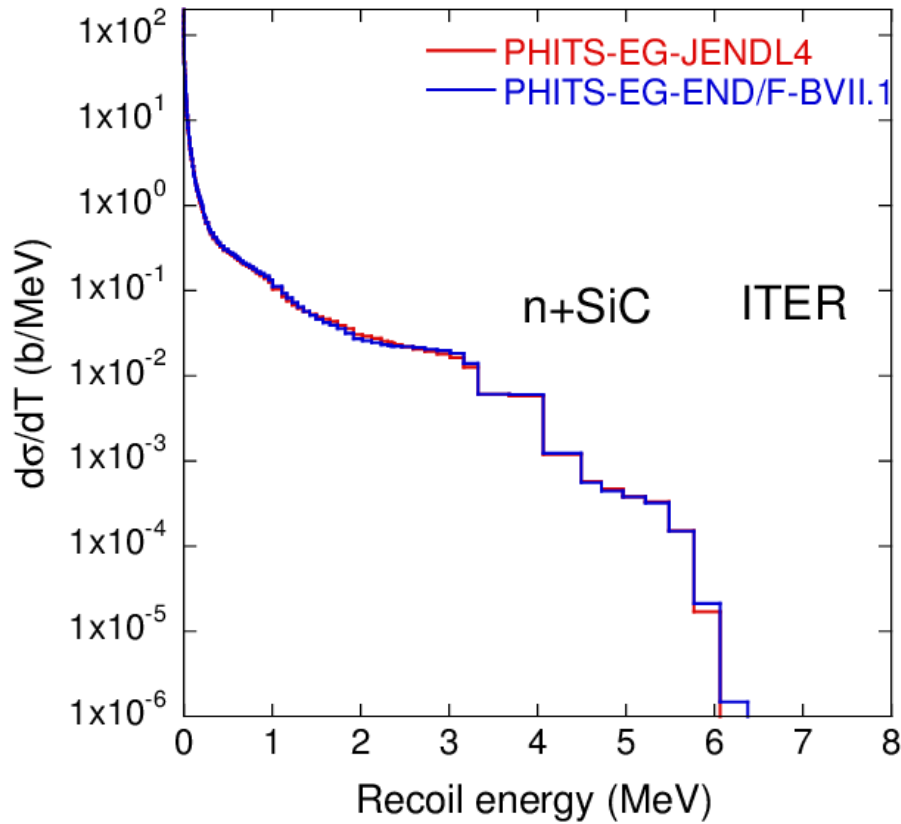


SPKA-ENDF/B-VII.1 is close to SPKA-JENDL4 below 0.6 MeV.

PKA spectra for $n+^{90}\text{Zr}$

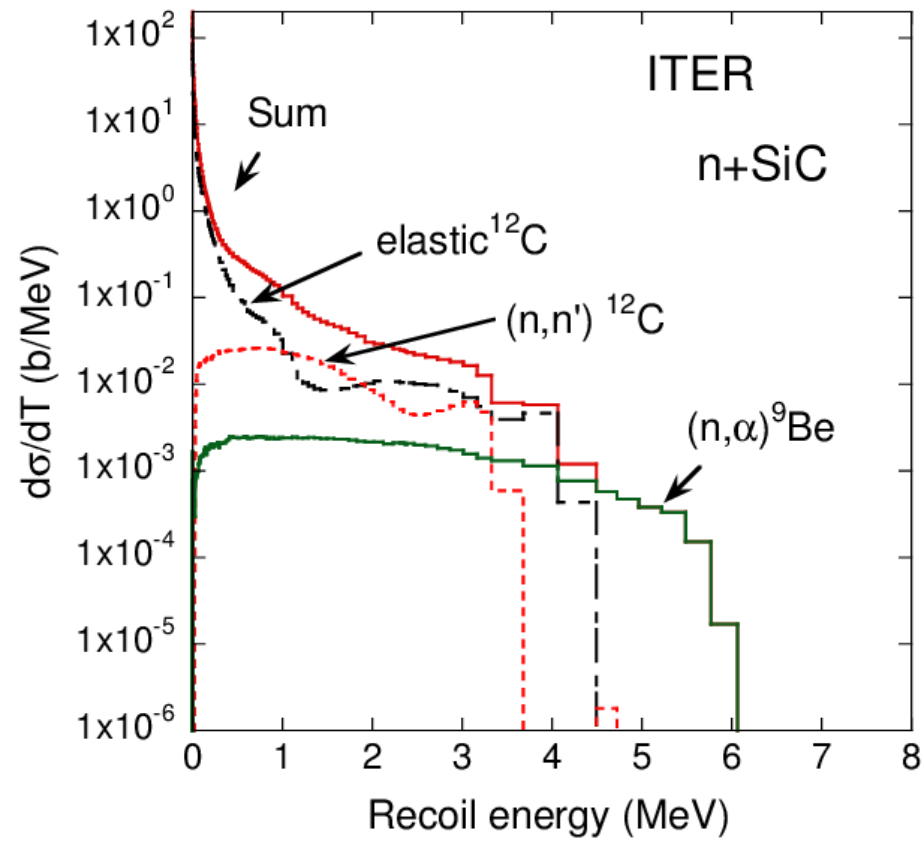
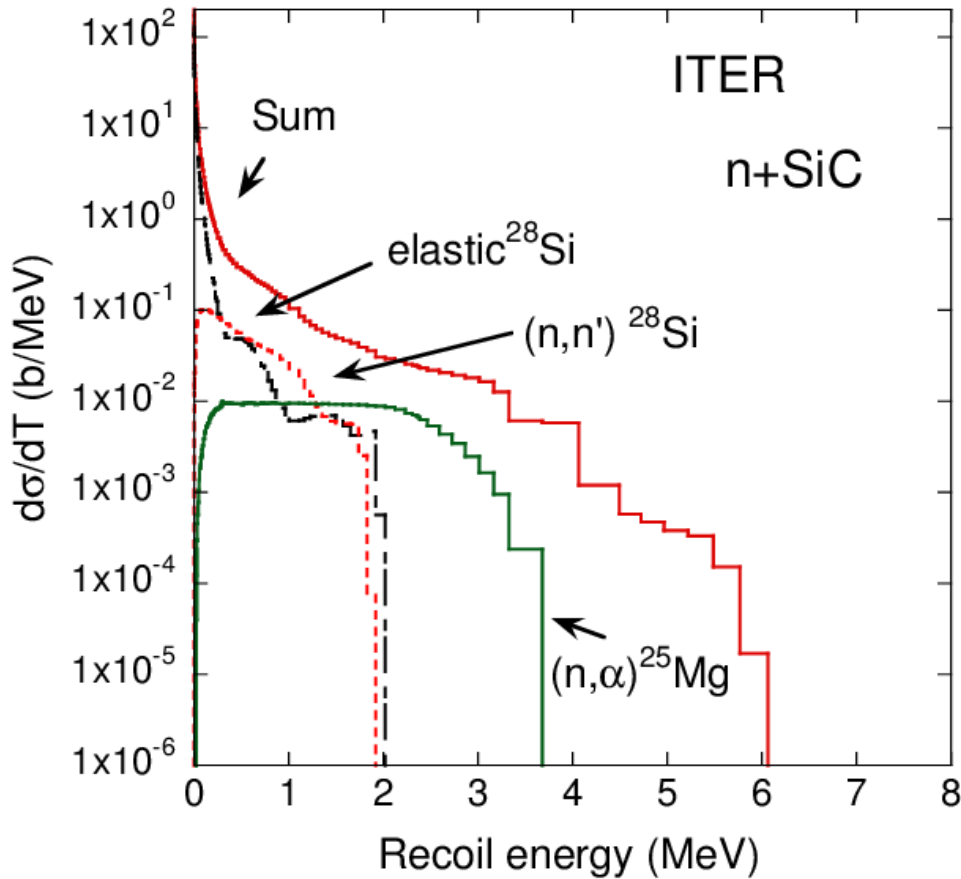


PKA spectra for n+SiC

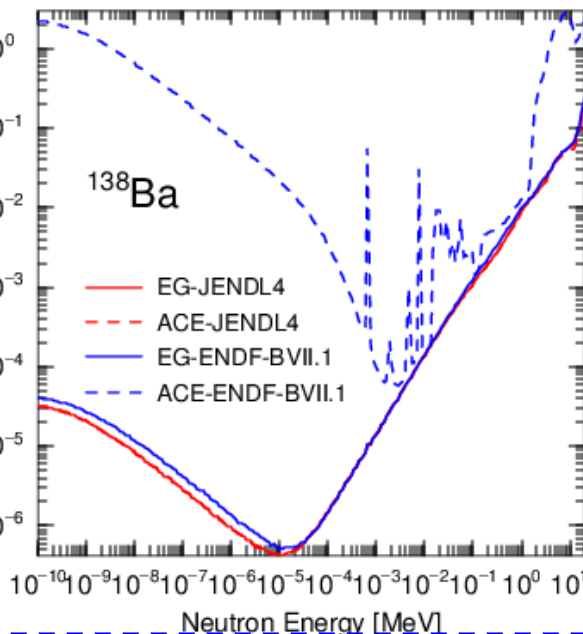
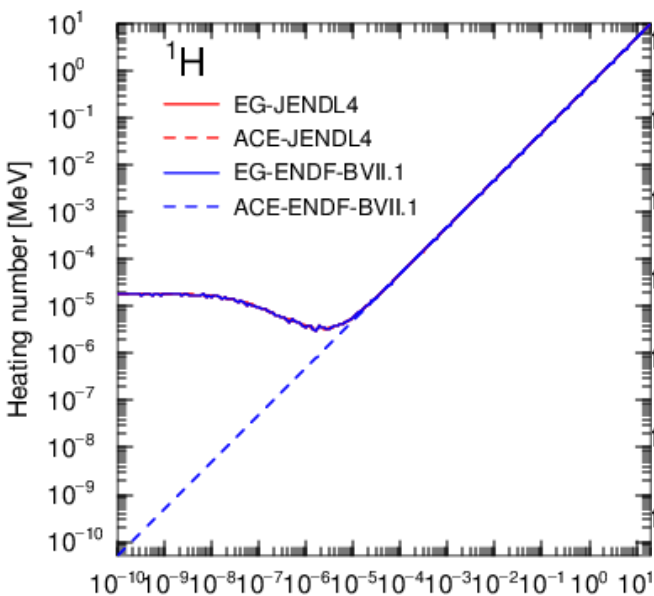


Good agreements between PHITSEG-JENDL4
and PHITS EG-ENDF/BVII.1.

PKA spectra for n+SiC

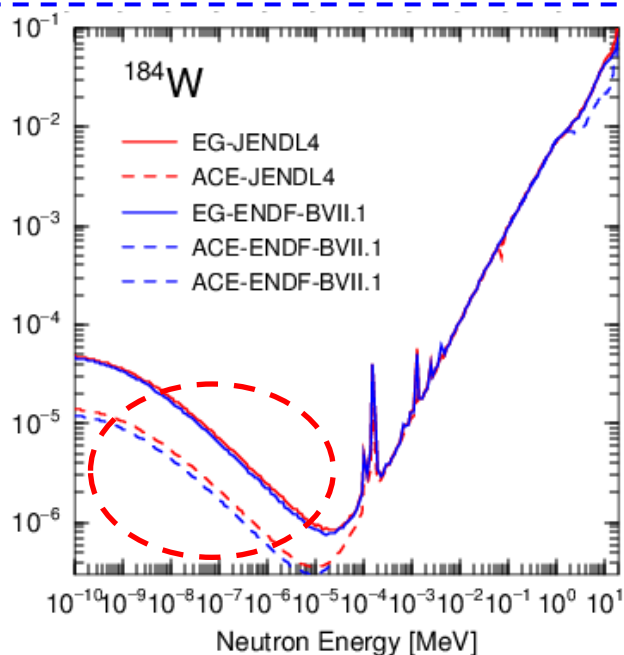


Comparison of calculated results with values in ACE files



• PHITS-EG:
Not give strange results.

PHITS-EG results are good agreements with value in ACE file of JENDL4.



• neutron capture reaction:
EGとNJOYの反跳核エネルギー導出の違いが原因か。

運動学: $E_{\gamma} = 5$ MeVとすると、 ^{185}W の反跳エネルギー72 eV

NJOYのエネルギーバランス:

$$k_{ij}(E) = (E + Q_{ij} - \bar{E}_{ijn} - \bar{E}_{ij\gamma}) \sigma_{ij}(E)$$

極めて大きな数の差し引き

極めて精度が悪いと考えられる。